A DIAGRAMMATIC TEMPERLEY-LIEB CATEGORIFICATION

BEN ELIAS

Contents

Abstract. The monoidal category of Soergel bimodules categorifies the Hecke algebra of a finite Weyl group. In the case of the symmetric group, morphisms in this category can be drawn as graphs in the plane. We define a quotient category, also given in terms of planar graphs, which categorifies the Temperley-Lieb algebra. Certain ideals appearing in this quotient are related both to the 1-skeleton of the Coxeter complex and to the topology of 2D cobordisms. We demonstrate how further subquotients of this category will categorify the cell modules of the Temperley-Lieb algebra.

1. Introduction

The goal of the categorification theorist is to replace interesting endomorphisms of a vector space with interesting endofunctors of a category. The question is: what makes these functors interesting? In the pivotal paper of Chuang and Rouquier [4], a fresh paradigm emerged. They noticed that specifying structure on the natural transformations (morphisms) between these functors would force the categorification to be more "beautiful" (in this case, the added beauty was a useful derived equivalence). The categorification of quantum groups by Rouquier [17], Lauda [13], and Khovanov and Lauda [12] has shown that categorifying an algebra A (with a category $\mathcal{A}$) will specify just what this additional structure should be, for categorifications of every representation of that algebra: a functor from $\mathcal{A}$ to an endofunctor category. That their categorifications $\mathcal{A}$ provide the "correct" extra structure is confirmed by the fact that existing geometric categorifications conform to it (see [24]) and that all irreducibles of A can be categorified in this way (see [14]). The salient feature of these categorifications is that, instead of being defined abstractly, the morphisms are presented by generators and relations, making it straightforward to define functors out of $\mathcal{A}$.

In the case of the Hecke algebra $\mathcal{H}$, categorifications have existed for some time, in the guise of category $\mathcal{O}$ or perverse sheaves on the flag variety. In [18] Soergel rephrased these categorifications in a more combinatorial way, constructing an additive categorification of $\mathcal{H}$ by a certain full monoidal subcategory $\mathcal{HC}$ of graded R-bimodules, where R is the coordinate ring of the geometric representation. Objects in this full subcategory are called *Soergel bimodules*. There are deep connections between Soergel bimodules, representation theory, and geometry, and we refer the reader to [18, 19, 20, 21] for more details.

In [6], the author and M. Khovanov provide (in type A) a presentation of $\mathcal{H}$ by generators and relations, where morphisms can be viewed diagrammatically as decorated graphs in a plane. While there is not yet a description of the added beauty arising from this structure on categorifications of Hecke representations, one should expect this to be the "correct" categorification of the Hecke algebra due to its connection with geometry.

To be more precise, the diagrammatics are for a smaller category $\mathcal{HC}_1$, the (ungraded) category of *Bott-Samuelson bimodules*. Soergel bimodules are obtained from $\mathcal{HC}_1$ by taking the graded Karoubi envelope. This is in exact analogy with the procedures of Khovanov and Lauda in [12].

The Temperley-Lieb algebra $\mathcal{TL}$ is a well-known quotient of $\mathcal{H}$, and it can be categorified by a quotient $\mathcal{TLC}$ of $\mathcal{HC}$, as this paper endeavors to show. Thus we have a naturally arising categorification by generators and relations, and we expect it to be a useful one. We will discuss this below. Objects in $\mathcal{TLC}$ can no longer be viewed as R-bimodules, though their Hom spaces will be R-bimodules.

The quotient category $\mathcal{TLC}$ is easy to describe diagrammatically in its own right, since the most complicated generator of $\mathcal{HC}$ is killed in the quotient. Take a category where objects are sequences of indices between 1 and n, viewed as colored points on the real number line (where each index is assigned a "color"). Morphisms will be

given by a collection of graphs embedded in $\mathbb{R} \times [0,1]$, one for each color, such that the graphs have only trivalent or univalent vertices, and such that the graph colored i and the graph colored $i+1$ are disjoint. The intersection of the graph with $\mathbb{R} \times \{0\}$ and $\mathbb{R} \times \{1\}$ determine the source and target objects respectively. Finally, some local graphical relations are imposed on these morphisms. This defines $\mathcal{TLC}_1$, and we take the graded Karoubi envelope to obtain $\mathcal{TLC}$.

We also provide a diagrammatic categorification of all the cell modules of $\mathcal{TL}$, as well as certain induced representations, in a fashion analogous to quantum group categorifications. Having found a diagrammatic categorification $\mathcal{C}$ of the positive half of the quantum group, Khovanov and Lauda in [11] conjectured that highest weight modules (naturally quotients of the positive half) could be categorified by quotients of $\mathcal{C}$ by the appearance of certain pictures on the *left*. This approach was proven correct by Lauda and Vazirani [14], and then used by Webster to categorify tensor products [26]. For the Temperley-Lieb algebra, the indecomposables (i.e. cell modules) are easiest described not as quotients but as subquotients of $\mathcal{TL}$. We categorify the subquotient by modding out our diagrammatics by the appearance of certain colors on the left, and then taking a full subcategory. A future paper will explore how this procedure can yield a large number of induced representations.

The proof that $\mathcal{TLC}$ categorifies $\mathcal{TL}$ uses a method similar to that in [6]. We show first that $\mathcal{TLC}$ is a *potential categorification*, that is, there is a surjective map from $\mathcal{TL}$ to $K(\mathcal{TLC})$. This defines a pairing on $\mathcal{TL}$ given by $([M],[N]) = \text{gdimHOM}(M,N)$, or equivalently a trace on $\mathcal{TL}$ via $\varepsilon([M]) = \text{gdimHOM}(\mathbb{1}, M)$ where $\mathbb{1}$ is the monoidal identity. There is a convenient set of elements in $\mathcal{TL}$ whose values uniquely and freely determine any pairing; hence, there is a convenient set of objects such that knowing their Hom spaces will imply that one knows all Hom spaces. In fact, these select Hom spaces will all be rings, and quotients of R. We use graphical methods to determine the graded rank of these rings, and show that they are not too small (since a priori, the quotient category could be zero). Similarly, the subquotient categories induce a pairing on the subquotient representations, which we calculate graphically on convenient elements. Once one has shown that the Hom spaces in $\mathcal{TLC}$ induce a nice trace/pairing on $\mathcal{TL}$, proving that the map $\mathcal{TL} \to K(\mathcal{TLC})$ is injective is easy. See Section 3.2 for details.

Let V be the geometric representation of S_{n+1}. We call a line in V a *Weyl line* if it is cut out by a transverse intersection of reflection-fixed hyperplanes. Let $Z \subset V$ be the union of all *Weyl lines*. One might intuitively expect a connection between Z and the Temperley-Lieb algebra, because of the avoidance of higher parabolic subgroups. It turns out that Hom spaces in $\mathcal{TLC}$ are supported on Z, or in other words, they are R/I bimodules where I is the vanishing ideal of Z. Hom spaces may be supported on subvarieties $Z' \subset Z$, where Z' is the union of those Weyl lines satisfying an appropriate transverseness property. The rings of the previous paragraph will be the coordinate rings of such Z'.

This paper is reasonably self-contained. We do not require familiarity with [6]. The difficult graphical arguments of that paper can often be drastically simplified for the

Temperley-Lieb setting, and we provide easier proofs for the results we need. Familiarity with diagrammatics for monoidal categories with adjunction would be useful. More details on such preliminary topics can be found in [6].

We now ask in what sense this categorification is interesting.

Soergel bimodules are intrinsically linked with braids, as was shown by Rouquier in [15, 16]. As such, morphisms between Soergel bimodules should correspond roughly to movies, and the graphs appearing in the diagrammatic presentation of the category $\mathcal{HC}$ should be (heuristically) viewed as 2-dimensional holograms of braid cobordisms. This is studied in [7]. The Temperley-Lieb quotient is associated with the representation theory of $U_q(\mathfrak{sl}_2)$, for which braids all degenerate into 1-manifolds, and braid cobordisms degenerate into surfaces with disorientations. There is a functor $\mathcal{F}$ from $\mathcal{TLC}$ to the category of disorientations constructed by Vaz [25]. We believe it is clear that the functor $\mathcal{F}$ is faithful (though certainly not full), and remark on this below in 3.6. This in turn yields a topological motivation of the variety Z and its subvarieties Z'. Because $\mathcal{F}$ is not full, there might be actions of $\mathcal{TLC}$ that do not extend to actions of disoriented cobordisms.

Categorification and the Temperley-Lieb algebra have a long history. Khovanov in [10] constructed a categorification of $\mathcal{TL}$ using a TQFT, which was slightly generalized by Bar-Natan in [3]. This was then used to categorify the Jones polynomial. Bernstein, Frenkel and Khovanov in [2] provide a categorical action of the Temperley-Lieb algebra by Zuckerman and projective functors on category $\mathcal{O}$. Stroppel [23] showed that this categorical action extends to the full tangle algebroid, but more importantly in our context, she also investigated the natural transformations between projective functors, and constructed a projective action of the cobordism category using these natural transformations. To study natural transformations she used Soergel's functor and calculations on Soergel bimodules. From this, it should not be terribly difficult to verify whether the category defined in this paper acts by projective functors. In some sense, cobordisms have always provided a reasonable notion for the structure of natural transformations in Temperley-Lieb categorical actions, though we would argue that the category $\mathcal{TLC}$ is more explicit and easier to use, being inherently planar, graph-theoretical, and having Hom spaces whose size is well-understood.

The organization of this paper is as follows. Chapter 2 will provide a quick overview of the Hecke and Temperley-Lieb algebras, and the diagrammatic definition of the category $\mathcal{HC}$. Chapter 3 begins by defining the quotient category diagrammatically in its own right (which makes a thorough understanding of the diagrammatic calculus for $\mathcal{HC}$ unnecessary). Section 3.2 states and proves the main theorem, modulo the lemma which requires all the work. The remaining sections of that chapter do all the work, and starting with Section 3.5 one will not miss any important ideas if one skips the proofs. Chapter 4 begins with a discussion of cell modules for $\mathcal{TL}$ and certain other modules, and then goes on to categorify these modules, requiring only very simple diagrammatic arguments.

Acknowledgments.

The author was supported by NSF grants DMS-524460 and DMS-524124, and would like to thank Mikhail Khovanov for his suggestions.

2. Preliminaries

Fix $n \in \mathbb{N}$, and let $I = 1, \ldots, n$ index the vertices of the Dynkin diagram A_n. We use the word *index* for an element of I, and the letters i, j always represent indices. Indices $i \neq j$ are *adjacent* if $|i-j| = 1$, and *distant* if $|i-j| \geq 2$, and questions of adjacency always refer to the Dynkin diagram, not the position of indices in a word or picture.

We will assign a color to each index, and speak of indices and colors interchangeably. Colors will usually represent generic indices, subject to specified adjacency relations.

Let $W = S_{n+1}$ with simple reflections $s_i = (i, i+1)$. Let $\Bbbk$ be a field of characteristic not dividing $2(n+1)$. Let $R = \Bbbk[x_1, \ldots, x_{n+1}]/e_1$, where $e_1 = x_1 + x_2 + \ldots + x_{n+1}$. R is a graded ring, with $\deg(x_i) = 2$, and is the coordinate ring of the geometric representation of W. We will abuse notation and refer to elements of $\Bbbk[x_1, \ldots, x_{n+1}]$ and their images in R in the same way, and will refer to both as polynomials. Note that $R = \Bbbk[f_1, \ldots, f_n]$ where $f_i = x_i - x_{i+1}$, since $x_1 = \frac{nf_1 + (n-1)f_2 + \ldots + f_n}{n+1}$ modulo e_1.

There is an obvious action of S_{n+1} on R, which permutes the generators x_i. There is a map ∂_i of degree -2 from R to the invariant ring R^{s_i}, sending f to $\frac{f - s_i(f)}{x_i - x_{i+1}}$, which is R^{s_i}-linear, and sends R^{s_i} to 0.

We always use the word *trace* to designate a $\mathbb{Z}[t, t^{-1}]$-linear map $\varepsilon \colon A \to \mathbb{Z}[[t, t^{-1}]]$, where A is a $\mathbb{Z}[t, t^{-1}]$-algebra, satisfying $\varepsilon(xy) = \varepsilon(yx)$. Let $\overline{(\cdot)}$ be the $\mathbb{Z}$-linear involution of $\mathbb{Z}[t, t^{-1}]$ sending t to t^{-1}. We call an operation on a $\mathbb{Z}[t, t^{-1}]$-algebra *t-antilinear* if it is $\mathbb{Z}[t, t^{-1}]$-linear after twisting by $\overline{(\cdot)}$. We write $[2] \stackrel{\text{def}}{=} t + t^{-1}$.

2.1. The Hecke Algebra and the Soergel Categorification.

For Soergel's original definition see [18], and for an easier version, see [21]. For more details, see [6].

The Hecke algebra $\mathcal{H}$ for S_{n+1} has a presentation as an algebra over $\mathbb{Z}[t, t^{-1}]$ with generators b_i, $i = 1, \ldots, n$ and the *Hecke relations*

$$b_i^2 = (t + t^{-1}) b_i \tag{2.1}$$

$$b_i b_j = b_j b_i \quad \text{for distant } i, j \tag{2.2}$$

$$b_i b_j b_i + b_j = b_j b_i b_j + b_i \text{ for adjacent } i, j. \tag{2.3}$$

Let us call the category of Bott-Samuelson bimodules $\mathcal{HC}_1$. It is a full monoidal subcategory of R-bimodules, whose objects are all free as left R-modules, and which is generated by certain objects B_i, $i \in I$. These objects satisfy

$$B_i \otimes B_i \cong B_i\{1\} \oplus B_i\{-1\} \tag{2.4}$$

$$B_i \otimes B_j \cong B_j \otimes B_i \text{ for distant } i, j \tag{2.5}$$

$$B_i \otimes B_j \otimes B_i \oplus B_j \cong B_j \otimes B_i \otimes B_j \oplus B_i \text{ for adjacent } i, j. \tag{2.6}$$

The Grothendieck group of $\mathcal{HC}_1$ (or rather, of its additive and grading closure, see below) is isomorphic to $\mathcal{H}$, with $[B_i]$ being sent to b_i, and $[R\{1\}]$ being sent to t.

We write the monomial $b_{i_1}b_{i_2}\cdots b_{i_d} \in \mathcal{H}$ as $b_{\underline{\boldsymbol{i}}}$ where $\underline{\boldsymbol{i}} = i_1 \dots i_d$ is a finite sequence of indices; by abuse of notation, we sometimes refer to this monomial simply as $\underline{\boldsymbol{i}}$. If $\underline{\boldsymbol{i}}$ is as above, we say the monomial has *length* d. We call a monomial *non-repeating* if $i_k \neq i_l$ for $k \neq l$, and *increasing* if $i_1 < i_2 < \dots$. The empty set is a sequence of length 0, and $b_\emptyset = 1$. Similarly, in $\mathcal{HC}_1$, write $B_{i_1} \otimes \dots \otimes B_{i_d}$ as $B_{\underline{\boldsymbol{i}}}$. Note that $B_\emptyset = R$, the monoidal identity. For an arbitrary index i and sequence $\underline{\boldsymbol{i}}$, we write $i \in \underline{\boldsymbol{i}}$ if i appears in $\underline{\boldsymbol{i}}$.

Each object in $\mathcal{HC}_1$ has a biadjoint with respect to $\otimes$, and B_i is self-biadjoint. Let ω be the t-antilinear anti-involution on $\mathcal{H}$ which fixes b_i, i.e. $\omega(t^a b_{\underline{\boldsymbol{i}}}) = t^{-a} b_{\sigma(\underline{\boldsymbol{i}})}$ where σ reverses the order of a sequence. Then the contravariant functor sending an object to its biadjoint will descend on the Grothendieck group to ω.

A *pairing* is a $\mathbb{Z}$-linear map $(,)\colon \mathcal{H} \times \mathcal{H} \to \mathbb{Z}[[t, t^{-1}]]$ which satisfies two criteria: it is *semi-linear*, i.e. $(ax, y) = \overline{a}(x, y)$ while $(x, ay) = a(x, y)$, for $a \in \mathbb{Z}[t, t^{-1}]$; and b_i is self-adjoint, so that $(x, b_i y) = (b_i x, y)$ and $(x, y b_i) = (x b_i, y)$ for all $x, y \in \mathcal{H}$ and all $i \in I$. There is a bijection between pairings $(,)$ and traces ε, defined by letting $(x, y) = \varepsilon(\omega(x)y)$, or conversely $\varepsilon(y) = (1, y)$.

It is a fact that a trace/pairing is uniquely determined by the function $\pi\colon \{\text{Increasing Sequences } \underline{\boldsymbol{i}}\} \to \mathbb{Z}[[t, t^{-1}]]$ given by $\pi(\underline{\boldsymbol{i}}) = \varepsilon(\underline{\boldsymbol{i}}) = (1, \underline{\boldsymbol{i}})$. It is also true that $\varepsilon(\underline{\boldsymbol{j}}) = \pi(\underline{\boldsymbol{i}})$ when $\underline{\boldsymbol{j}}$ is non-repeating and $\underline{\boldsymbol{i}}$ is the increasing sequence which is a reordering of $\underline{\boldsymbol{j}}$, so that we may view π as a function on non-repeating sequences which is invariant under reordering. However, not every π extends to a well-defined trace ε. When there is ambiguity, we denote the pairing corresponding to π by $(,)_\pi$. We use the vector π to encode pairings because $\pi(\underline{\boldsymbol{i}})$ will later be calculated as the graded dimension of a ring associated to $\underline{\boldsymbol{i}}$.

Let us quickly explain why ε should be uniquely determined by π. Moving an index from the beginning of a monomial to the end, or vice versa, will be called *cycling* the monomial. It is clear, using biadjointness or the definition of trace, that the value of ε is invariant under cycling. It is not difficult to show that any monomial may be reduced, using cycling and the Hecke relations, to a linear combination of increasing monomials, and therefore ε is determined by these. This same argument works for the Temperley-Lieb algebra.

Consider the function π_{std} given by $\pi_{\text{std}}(\underline{\boldsymbol{i}}) = t^d$, where d is the length of $\underline{\boldsymbol{i}}$. It yields a well-defined pairing, and the corresponding trace map ε is well-known: it picks out the coefficient of the identity in the standard basis of $\mathcal{H}$. The pairing can be used to understand Hom spaces in $\mathcal{HC}_1$. Given objects M, N, let $\mathrm{HOM}(M, N) \stackrel{\text{def}}{=} \bigoplus_{m \in \mathbb{Z}} \mathrm{Hom}(M, N\{m\})$. Soergel showed that $\mathrm{HOM}(B_{\underline{\boldsymbol{i}}}, B_{\underline{\boldsymbol{j}}})$ is a *free* graded left (or right) R-module of rank $(b_{\underline{\boldsymbol{i}}}, b_{\underline{\boldsymbol{j}}})_{\pi_{\text{std}}}$. Let $\pi'_{\text{std}} = \frac{\pi_{\text{std}}}{(1-t^2)^n}$. Since the graded dimension of R as a $\Bbbk$-vector space is $\frac{1}{(1-t^2)^n}$ we have that the graded dimension of $\mathrm{HOM}(B_{\underline{\boldsymbol{i}}}, B_{\underline{\boldsymbol{j}}})$ is $(b_{\underline{\boldsymbol{i}}}, b_{\underline{\boldsymbol{j}}})_{\pi'_{\text{std}}}$.

Now let ε be the quotient map $A \to \mathbb{Z}[t, t^{-1}]$ by the ideal generated by all b_i. It is a homomorphism to a commutative algebra, so it is a trace. The corresponding pairing satisfies $(1,1) = 1$ and $(x,y) = 0$ for monomials x, y if either monomial is not 1. The corresponding function is π_{triv}, where $\pi_{\text{triv}}(\emptyset) = 1$ and $\pi_{\text{triv}}(\underline{\boldsymbol{i}}) = 0$ for any $\underline{\boldsymbol{i}} \neq \emptyset$.

The only traces we care about will be linear combinations of π_{std} and π_{triv}. However, for more information on traces, see [5].

2.2. **The Temperley-Lieb Algebra.** Relation (2.3) implies the equality $b_i b_{i+1} b_i - b_i = b_{i+1} b_i b_{i+1} - b_{i+1} \stackrel{\text{def}}{=} c_i$, for each $1 \leq i \leq n-1$. The Temperley-Lieb algebra $\mathcal{TL}$ is a quotient of $\mathcal{H}$ by the 2-sided ideal generated by all c_i. To avoid any ambiguity, we let $u_i, u_{\underline{\boldsymbol{i}}} \in \mathcal{TL}$ denote the images of $b_i, b_{\underline{\boldsymbol{i}}} \in \mathcal{H}$ in the quotient. Then $\mathcal{TL}$ is generated by u_i with the relations

$$u_i^2 = [2]\, u_i \tag{2.7}$$

$$u_i u_j = u_j u_i \text{ for } |i-j| \geq 2 \tag{2.8}$$

$$u_i u_{i+1} u_i = u_i \tag{2.9}$$

$$u_{i+1} u_i u_{i+1} = u_{i+1}. \tag{2.10}$$

A permutation $\sigma \in S_{n+1}$ is called *321-avoiding* if it never happens that, for $i < j < k$, $\sigma(i) > \sigma(j) > \sigma(k)$. It turns out that, using the Temperley-Lieb relations, every monomial $u_{\underline{\boldsymbol{j}}}$ is equal to a scalar times some $u_{\underline{\boldsymbol{i}}}$ where $\underline{\boldsymbol{i}}$ is *321-avoiding*, i.e. if viewed as a word in the symmetric group it represents a *reduced* expression for a 321-avoiding permutation. Moreover, between 321-avoiding monomials, the only further relations come from (2.8), and hence it is easy to pick out a basis from this spanning set.

The Temperley-Lieb algebra has a well-known topological interpretation, thanks to Kauffman [9]. We skim over it here; see [27] for a longer exposition. An element of $\mathcal{TL}$ is a linear combination of crossingless matchings (isotopy classes of embedded planar 1-manifolds) between $n+1$ bottom points and $n+1$ top points. Multiplication of crossingless matchings consists of vertical concatenation, followed by removing any circles and replacing them with a factor of [2]. In this picture, u_i becomes the following:

Any increasing monomial is 321-avoiding. Increasing monomials are easy to visualize topologically, as they have only "left-leaning lines" and "simple cups and caps." For example:

$u_1 u_2 u_3 u_6 u_7 u_9 \mapsto$ 

Any trace ε on $\mathcal{TL}$ will be determined on increasing monomials $\underline{\boldsymbol{i}}$, and we encode ε by the function on increasing monomials $\psi(\underline{\boldsymbol{i}}) \stackrel{\text{def}}{=} \varepsilon(\underline{\boldsymbol{i}})$.

Given a crossingless matching, its *closure* is a configuration of circles in the punctured plane obtained by wrapping the top boundary around the puncture to close up with the bottom boundary. See Section 3.2 for a picture. Circle configurations have two

topological invariants: the number of circles and the *nesting number*, which is the number of circles which surround the puncture, and is equal to $n+1-2k \geq 0$ for some $k \geq 0$. Given a scaling factor for each possible nesting number, one constructs a trace by letting $\varepsilon(u_{\underline{\boldsymbol{i}}}) = c\,[2]^m$ where m is the number of circles in the closure of $u_{\underline{\boldsymbol{i}}}$ and c is the scaling factor associated to its nesting number. To calculate (x, y), we place y below an upside-down copy of x (or vice versa), and then take the closure. All pairings/traces can be constructed this way, so they are all topological in nature. Again, for more information on traces see [5].

The Temperley-Lieb algebra has a *standard pairing* ψ_{std} of its own, which involves no rescaling: $\varepsilon(u_{\underline{\boldsymbol{i}}}) = [2]^m$ as above. One can check that $\psi_{\text{std}}(\underline{\boldsymbol{i}}) = [2]^{n+1-d}$ for an increasing monomial. This is *not* related to π_{std}, which does not descend to $\mathcal{TL}$. On the other hand, π_{triv} clearly does descend to a pairing ψ_{triv} on $\mathcal{TL}$, which only evaluates to a non-zero number when the nesting number is $n+1$.

It turns out that the pairing on $\mathcal{TL}$ arising from our categorification will satisfy $(1,1) = \frac{t^n}{(1-t^2)}\,[2]^n - \frac{t^2}{(1-t^2)}$ and $(1, u_{\underline{\boldsymbol{i}}}) = \frac{t^n}{(1-t^2)}\,[2]^{n-d}$. We will call this form ψ_0. Clearly $\psi_0 = \frac{t^n}{(1-t^2)[2]}\psi_{\text{std}} - \frac{t^2}{(1-t^2)}\psi_{\text{triv}}$. In particular, on any monomial $x \neq 1$, our trace will agree with a rescaling of the standard trace. When $n = 1$, the algebras $\mathcal{TL}$ and $\mathcal{H}$ are already isomorphic, and $\pi'_{\text{std}} = \psi_0$.

2.3. **Soergel Diagrammatics.** We now give an alternate description of the category $\mathcal{HC}_1$. What follows is a simplified version of the summary in [7].

An object in $\mathcal{HC}_1$ is given by a sequence of indices $\underline{\boldsymbol{i}}$, which is visualized as d points on the real line $\mathbb{R}$, labelled or "colored" by the indices in order from left to right. These objects are also called $B_{\underline{\boldsymbol{i}}}$. Morphisms are glued together from the following pictures, which may exist in various colors but with restrictions based on adjacency conditions.

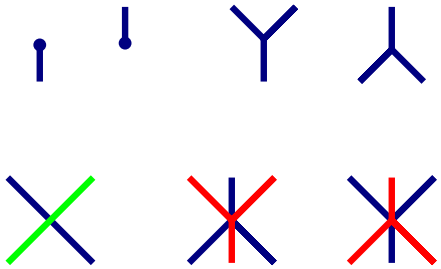

More precisely, a morphism is an embedding of a planar graph in $\mathbb{R} \times [0,1]$, *modulo isotopy*, satisfying the following properties:

(1) Edges of the graph are colored by indices from 1 to n.
(2) Edges may run into the boundary $\mathbb{R} \times \{0,1\}$, yielding two sequences of colored points on $\mathbb{R}$, the top boundary $\underline{\boldsymbol{i}}$ and the bottom boundary $\underline{\boldsymbol{j}}$. In this case, the graph is viewed as a morphism from $\underline{\boldsymbol{j}}$ to $\underline{\boldsymbol{i}}$.
(3) Only four types of vertices exist in this graph: univalent vertices or "dots", trivalent vertices with all three adjoining edges of the same color, 4-valent vertices

whose adjoining edges alternate in colors between i and j distant, and 6-valent vertices whose adjoining edges alternate between i and j adjacent.

The degree of a graph is +1 for each dot and -1 for each trivalent vertex. 4-valent and 6-valent vertices are of degree 0.

For instance, if "blue" corresponds to the index i and "red" to j, then the lower right generator is a degree 0 morphism from jij to iji.

As usual in a diagrammatic category, composition of morphisms is given by vertical concatenation, and the monoidal structure is given by horizontal concatenation.

We then allow $\Bbbk$-linear sums of graphs, and apply the relations below to obtain the category $\mathcal{HC}_1$. Some of these relations are redundant.

The relations are given in terms of colored pictures, but with no explicit assignment of indices to colors. They hold for *any* assignment of indices to colors, so long as certain adjacency conditions hold (for instance, red and blue above must be assigned to adjacent indices). We will specify adjacency for all pictures, although one can generally deduce it from the fact that 6-valent vertices only join adjacent colors, and 4-valent vertices only join distant colors.

For example, these first four relations hold, with blue representing a generic index.

(2.11)

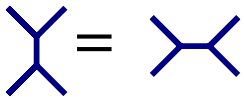

(2.12)

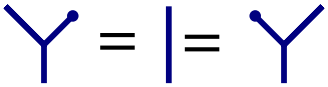

(2.13)

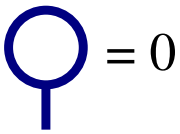

(2.14)

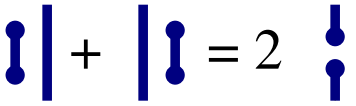

We will repeatedly call a picture looking like (2.13) by the name "needle." Note that a needle is not necessarily zero if there is something in the interior. A circle is just a needle with a dot attached, using (2.12), so it can be thought of as part of a graph.

Remark 2.1. It is an immediate consequence of relations (2.11) and (2.12) that any *tree* (graph without cycles) of one color is equal to:

- If it has no boundary, two dots connected by an edge. Call this a *double dot*.
- If it has one boundary edge, a single dot connected to the boundary. Call this a *boundary dot*.

- If it has more boundary edges, a tree with no dots and the fewest possible number of trivalent vertices needed to connect the boundaries. Moreover, any two such trees are equal. Call this a *simple tree*.

We refer to this as *tree reduction*.

Notation 2.2. Fix a color (blue). In a multicolored graph, we will still refer to part of that graph which is a blue simple tree as a simple tree, even if other colors are overlaid. However, we only use the terms boundary dot and double dot when that connected component of the graph does not meet any other colors. We may refer to a boundary dot (possibly with other colors overlaid) as a simple tree with one boundary edge, and an empty graph as a simple tree with zero boundary edges.

In the following relations, the two colors are distant.

(2.15) 

(2.16) 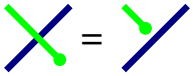

(2.17) 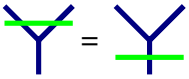

(2.18) 

In this relation, two colors are adjacent, and both distant to the third color.

(2.19) 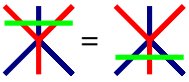

In this relation, all three colors are mutually distant.

(2.20) 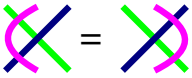

Remark 2.3. Relations (2.15) thru (2.20) indicate that any part of the graph colored i and any part of the graph colored j "do not interact" for i and j distant. That is, one may visualize sliding the j-colored part past the i-colored part, and it will not change the morphism. We call this the *distant sliding property*.

In the following relations, the two colors are adjacent.

(2.21) 

(2.22)

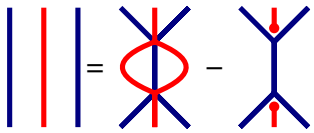

(2.23)

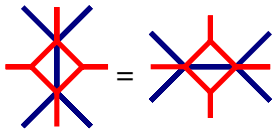

(2.24)

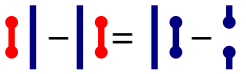

In this final relation, the colors have the same adjacency as $\{1, 2, 3\}$.

(2.25)

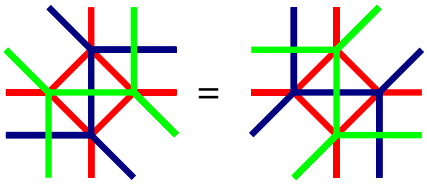

This concludes the definition of $\mathcal{HC}_1$. Note that $\mathcal{HC}_1$ is not even an additive category, although Hom spaces are graded $\mathbb{Z}$-modules. Before defining $\mathcal{HC}$ itself, we provide some commentary.

Relations (2.14), (2.24), and (2.18) are referred to as *dot forcing rules*, because they describe at what price one can "force" a double dot to the other side of a line. The three relations imply that, given a line and an arbitrary collection of double dots on the left side of that line, one can express the morphism as a sum of diagrams where all double dots are on the right side, or where the line is "broken."

We will occasionally use a shorthand to represent double dots. We identify a double dot colored i with the polynomial $f_i \in R$, and to a linear combination of disjoint unions of double dots in the same region of a graph, we associate the appropriate linear combination of products of f_i. For any polynomial $f \in R$, a square box with a polynomial f in a region will represent the corresponding linear combination of graphs with double dots.

For instance, 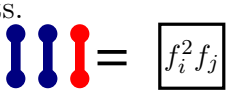 $= \boxed{f_i^2 f_j}$.

The implication of the dot forcing rules is that for any polynomial f, there exist polynomials g and h such that

(2.26)

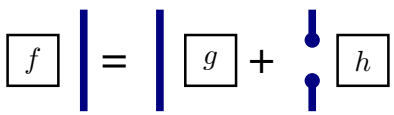

The polynomials appearing can be found using the map ∂_i, and in particular, $h = \partial_i(f)$. One particular implication is that

(2.27)

whenever f is a polynomial invariant under s_i (and blue represents i). As an exercise, the reader can check that f_i^2 slides through a line colored i.

We have an bimodule action of R on morphisms by placing boxes (i.e. double dots) in the leftmost or rightmost regions of a graph.

There is a functor from this diagrammatically defined category to the category of R-bimodules, whereby a diagram unambiguously represents a specific bimodule map. The functor preserves the left and right R action on morphisms.

Theorem 1 (Main Theorem of [6])**.** *There is an equivalence of categories between this diagrammatic category and $\mathcal{HC}_1$, the category of Bott-Samuelson bimodules.*

This does help to show what is less obvious in the diagrammatic context: that the R-bimodules $\mathrm{HOM}(M,N)$ are free as left or right R-modules. Besides this, we will not need any details about the bimodule version of $\mathcal{HC}_1$.

The following theorem and corollary are the most important results from [6], the crucial facts which allow all other proofs to work.

Theorem 2. (Color Reduction) *Consider a morphism $\varphi\colon \emptyset \to \underline{\boldsymbol{i}}$, and suppose that the index i (blue) appears in $\underline{\boldsymbol{i}}$ zero times (respectively: once). Then φ is in the $\Bbbk$-span of graphs which only contain blue in the form of double dots in the leftmost region of the graph (respectively: as well as a single boundary dot). This result may be obtained simultaneously for multiple indices i.*

Corollary 2.4. *The space $\mathrm{HOM}_{\mathcal{HC}_1}(\emptyset,\emptyset)$ is precisely R, viewed as a graded ring, and as a bimodule. In other words, it is freely generated over double dots by the empty diagram.*

The space $\mathrm{HOM}_{\mathcal{SC}_1}(\emptyset,\underline{\boldsymbol{i}})$ for $\underline{\boldsymbol{i}}$ non-repeating is a free (left, or right) R-module of rank 1, generated by the following morphism of degree d.

The proofs of these statements do not use any sophisticated technology, only convoluted pictorial arguments, and comprise the bulk of [6]. We will not need to quote these results, as we will show the equivalent results for $\mathcal{TLC}$ easily.

Finally, let us consider where the isomorphisms (2.4) through (2.6) come from. We have the following implication of (2.14):

(2.28)

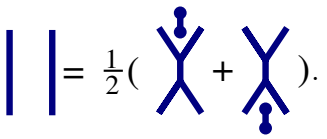

The identity id_{ii} decomposes as a sum of two orthogonal idempotents, each of which is the composition of a "projection" and an "inclusion" map of degree ± 1, to and from B_i (explicitly, $\mathrm{id}_{ii} = i_1 p_1 + i_2 p_2$ where $p_1 i_1 = \mathrm{id}_i$, $p_2 i_2 = \mathrm{id}_i$, $p_1 i_2 = 0 = p_2 i_1$). This implies (2.4), and is a typical example of how direct sum decompositions work in diagrammatic categories.

Relation (2.15) immediately implies (2.5).

To obtain (2.6), we must be more sophisticated.

Given a category $\mathcal{C}$ whose morphism spaces are $\mathbb{Z}$-modules, we may take its *additive closure*, which formally adds direct sums of objects, and yields an additive category. Given $\mathcal{C}$ whose morphism spaces are graded $\mathbb{Z}$-modules, we may take its *grading closure*, which formally adds shifts of objects, but restricts morphisms to be homogeneous of degree 0. Given $\mathcal{C}$ an additive category, one may take the *idempotent completion* or *Karoubi envelope*, which formally adds direct *summands*. Recall that the Karoubi envelope has as objects pairs (B, e) where B is an object in $\mathcal{C}$ and e an idempotent endomorphism of B. This object acts as though it were the "image" of this projection e, and behaves like a direct summand. When taking the Karoubi envelope of a graded category (or a category with graded morphisms) one restricts to homogeneous degree 0 idempotents. We refer in this paper to the entire process which takes a category $\mathcal{C}$, whose morphism spaces are graded $\mathbb{Z}$-modules, and returns the Karoubi envelope of its additive and grading closure as taking the *graded Karoubi envelope*. All these transformations can interact nicely with monoidal structures. We let $\mathcal{HC}$ be the graded Karoubi envelope of $\mathcal{HC}_1$. For sake of discussion, we let $\mathcal{HC}_2$ be the additive grading closure of $\mathcal{HC}_1$.

The two color variants of relation (2.22) together express the direct sum decompositions

$$B_i \otimes B_{i+1} \otimes B_i = C_i \oplus B_i \tag{2.29}$$

$$B_{i+1} \otimes B_i \otimes B_{i+1} = C_i \oplus B_{i+1}. \tag{2.30}$$

Again, the identity $\mathrm{id}_{i(i+1)i}$ is decomposed into orthogonal idempotents. The second idempotent factors through B_i, and the corresponding object in the Karoubi envelope will be isomorphic to B_i. The first idempotent, which we call a "doubled 6-valent vertex," corresponds to a new object in the idempotent completion. It turns out that the doubled 6-valent vertex for "blue red blue" is isomorphic in the Karoubi envelope to the doubled 6-valent vertex for "red blue red" (i.e. their images are isomorphic), so by abuse of notation we call both these new objects C_i. It is a summand of both $i(i+1)i$ and $(i+1)i(i+1)$. The image of C_i in the Grothendieck group is c_i.

2.4. **Aside on Karoubi Envelopes and Quotients.** If $\mathcal{C}$ is a full subcategory of (graded) R-bimodules for some ring R, then the transformations described above behave as one would expect them to. In particular, the Karoubi envelope agrees with the full subcategory which includes all summands of the previous objects. The Grothendieck group of the Karoubi envelope is in some sense "under control," if one understands

indecomposable R-bimodules already. On the other hand, the Karoubi envelope of an arbitrary additive category may be enormous, and to control the size of its Grothendieck group one should understand and classify all idempotents in the category, a serious task. Also, arbitrary additive categories need not have the Krull-Schmidt property, making their Grothendieck groups even more complicated.

The Temperley-Lieb algebra is obtained from the Hecke algebra by setting the elements c_i to zero, for $i = 1, \dots, n-1$. These elements lift in the Soergel categorification to objects C_i. The obvious way one might hope to categorify $\mathcal{TL}$ would be to take the quotient of the category $\mathcal{HC}$ by each object C_i.

To mod out an additive *monoidal* category $\mathcal{C}$ by an object Z, one must kill the *2-dimensional* ideal of id_Z in $\mathrm{Mor}(\mathcal{C})$. That is, the morphism space $\mathrm{Hom}(X, Y)$ in the quotient category is exactly $\mathrm{Hom}_{\mathcal{C}}(X, Y)$ modulo the submodule of morphisms factoring through $V \otimes Z \otimes W$ for any V, W. If the category is drawn diagrammatically, one need only kill any diagram which has id_Z as a subdiagram.

We have not truly drawn $\mathcal{HC}$ diagrammatically, only $\mathcal{HC}_1$. The object we wish to kill is not an object in $\mathcal{HC}_1$; the closest thing we have is the corresponding idempotent, the doubled 6-valent vertex. However, this is not truly a problem, due to the following proposition, whose proof we leave to the reader.

Proposition 2.5. *Let $\mathcal{C}_1$ be an additive category, B an object in $\mathcal{C}_1$, and e an idempotent in $\mathrm{End}(B)$. Let $\mathcal{D}_1$ be the quotient of $\mathcal{C}_1$ by the morphism e. Let $\mathcal{C}$ and $\mathcal{D}$ be the respective Karoubi envelopes. Finally, let $\mathcal{D}'$ be the quotient of $\mathcal{C}$ by the identity of the object (B, e). Then there is a natural equivalence of categories from $\mathcal{D}$ to $\mathcal{D}'$.*

The analogous statement holds when one considers graded Karoubi envelopes.

Remark 2.6. The equivalence constructed in this way will not be an *isomorphism* of categories; $\mathcal{D}'$ has more objects. For instance, (B, e) and $(B, 0)$ are distinct (isomorphic) objects in $\mathcal{D}'$, but are the same object in $\mathcal{D}$.

So to categorify $\mathcal{TL}$ diagrammatically, one might wish to take the quotient of $\mathcal{HC}_1$ by the doubled 6-valent vertex, and then take the Karoubi envelope.

The quotient of $\mathcal{HC}_1$ will no longer be a category which embeds nicely as a full subcategory of bimodules. One might worry that Krull-Schmidt fails, or that to understand its Karoubi envelope one must classify all idempotents therein. Thankfully, our calculation of HOM spaces will imply easily that its graded additive closure has Krull-Schmidt and is *already* idempotent closed, so it is equivalent to its own Karoubi envelope (see Section 3.2).

3. The Quotient Category $\mathcal{TLC}$

3.1. **Definition of $\mathcal{TLC}$.** As discussed in the previous section, our desire is to take the quotient of $\mathcal{HC}_1$ by the doubled 6-valent vertex, and then take the graded Karoubi envelope.

An important consequence of relations (2.21) and (2.13) is that

(3.1) 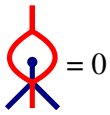

from which it follows, using (2.22), that

(3.2) 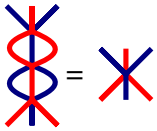

so the (monoidal) ideal generated in $\mathrm{Mor}(\mathcal{HC}_1)$ by a doubled 6-valent vertex is the same as the ideal generated by the 6-valent vertex.

Claim 3.1. *The following are all equivalent.*

(3.3) 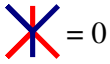

(3.4) 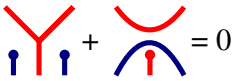

(3.5) 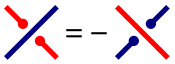

(3.6) 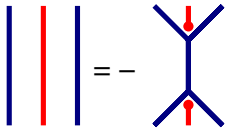

(3.7) 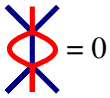

Proof. (3.3) $\Longrightarrow$ (3.4): Add a dot, and use relation (2.21). (3.4) $\Longrightarrow$ (3.5): Add a dot to the top. (3.5) $\Longrightarrow$ (3.4): Apply to the middle of the diagram. (3.5) $\Longrightarrow$ (3.6): Stretch dots from the blue strands towards the red strand, and then apply (3.5) to the middle. (3.6) $\Longrightarrow$ (3.7): Use relation (2.22). (3.7) $\Longrightarrow$ (3.3): Use (3.2). □

Modulo 6-valent vertices, the relations (2.21) and (2.22) become (3.4) and (3.6) above. All other relations involving 6-valent vertices, namely (2.23), (2.25), and (2.19), are sent to zero modulo 6-valent vertices. Relation (3.5) implies both (3.4) and (3.6) without reference to any graphs using 6-valent vertices. So if we wish to rephrase our quotient in terms of graphs that never have 6-valent vertices, the sole necessary relation imposed by the fact that 6-valent vertices were sent to zero is the relation (3.5).

Suppose we only allow ourselves univalent, trivalent, and 4-valent vertices, but no 6-valent vertices, in a graph Γ. Then the i-graph of Γ, which consists of all edges colored

i and all vertices they touch, will be disjoint from the $i+1$- and $i-1$-graphs of Γ. The distant sliding property implies that the i-graph and the j-graph of Γ effectively do not interact, when i and j are distant.

Thus we have motivated our graphical definition of $\mathcal{TLC}_1$. Objects will again be sequences of colored points on the line $\mathbb{R}$, which we will call $\underline{\boldsymbol{i}}$ or $U_{\underline{i}}$. Morphisms will be given (again, after linear combinations and some relations) by isotopy classes of the following data:

(1) For each i from 1 to n, a graph Γ_i embedded in the strip.
(2) Γ_i consists entirely of univalent and trivalent vertices, with edges (colored i) that may go to the boundary. Again, the intersection with the top and bottom boundary gives the target and source of the morphism, respectively.
(3) Γ_i and Γ_{i+1} are disjoint. All graphs Γ_i are pairwise disjoint on the boundary.

The degree of a graph is $+1$ for each dot and -1 for each trivalent vertex.

One may apply isotopy to each Γ_i individually, so long as it stays appropriately disjoint. Phrasing the definition in this fashion eliminates the need to add distant sliding rules, for these are now built into the notion of isotopy. Note that as we have stated it here, Γ_i and Γ_j may have edges which are embedded in a tangent fashion, or even entirely overlap. However, such embeddings are isotopic to graph embeddings with only transverse edge intersections, which arise as 4-valent vertices in our earlier viewpoint.

We then take $\Bbbk$-linear combinations of such graphs, and mod out by relations (2.11) through (2.14), (2.24) and the new relation (3.5) to get the morphisms in the category $\mathcal{TLC}_1$. As a reminder, the new relation is given here again.

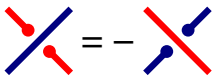

That this category is isomorphic to $\mathcal{HC}_1$ modulo the 6-valent vertex is obvious.

Remark 3.2. Note that tree reduction (see Remark 2.1) can now be applied to any tree of a single color in $\mathcal{TLC}$, regardless of what other colors are present, since the only colors which can intersect the tree are distant colors, which do not actually interfere.

We denote by $\mathcal{TLC}$ the graded Karoubi envelope of $\mathcal{TLC}_1$. However, we will show in the next section that the graded additive closure $\mathcal{TLC}_2$ of $\mathcal{TLC}_1$ is already idempotent-closed, so that $\mathcal{TLC}_2$ and $\mathcal{TLC}$ are the same.

It is obvious that

$$U_i \otimes U_{i+1} \otimes U_i \cong U_i \tag{3.8}$$

$$U_{i+1} \otimes U_i \otimes U_{i+1} \cong U_{i+1} \tag{3.9}$$

in $\mathcal{TLC}_1$, from the relation (3.6) and the simple calculation (using dot forcing rules) that

(3.10)

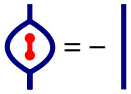

In particular, there is a map from $\mathcal{TL}$ to the split Grothendieck ring of $\mathcal{TLC}$, sending u_i to $[U_i]$. This induces a semi-linear pairing on $\mathcal{TL}$, via $(u_{\underline{\boldsymbol{i}}}, u_{\underline{\boldsymbol{j}}}) \stackrel{\text{def}}{=} \text{grkHOM}_{\mathcal{TLC}}(U_{\underline{\boldsymbol{i}}}, U_{\underline{\boldsymbol{j}}})$ where the graded rank is taken as a vector space over $\Bbbk$.

At this point, we have not shown that the category $\mathcal{TLC}$ is nonzero, so this pairing could be 0.

3.2. **Main Theorem.**

Theorem 3. *(Main Theorem) $\mathcal{TLC}_2$ has Krull-Schmidt and is idempotent-closed, so $\mathcal{TLC}_2 \cong \mathcal{TLC}$. $\mathcal{TLC}$ categorifies $\mathcal{TL}$.*

Lemma 3.3. *The pairing induced on $\mathcal{TL}$ from $\mathcal{TLC}_1$ is precisely given by ψ_0.*

That we can deduce the theorem from the lemma easily, in this small subsection, is an excellent illustration of the utility of fixing a semi-linear pairing on the base algebra and only considering categorifications which conform to it. Proving the lemma is a long and convoluted graphical argument.

In fact, we do not need any specifics about the category $\mathcal{TLC}_1$ in this argument, only that it is generated by objects U_i satisfying the categorified Temperley-Lieb relations and having the correct graded dimension of Hom spaces.

Proposition 3.4. *The object $U_{\underline{\boldsymbol{i}}}$ in $\mathcal{TLC}_1$ has no non-trivial (homogeneous) idempotents when $\underline{\boldsymbol{i}}$ is 321-avoiding. Moreover, if both $\underline{\boldsymbol{i}}$ and $\underline{\boldsymbol{j}}$ are 321-avoiding, then $U_{\underline{\boldsymbol{i}}} \cong U_{\underline{\boldsymbol{j}}}\{m\}$ in $\mathcal{TLC}_2$ if and only if $m = 0$ and $u_{\underline{\boldsymbol{i}}} = u_{\underline{\boldsymbol{j}}}$ in $\mathcal{TL}$.*

Proof. Two 321-avoiding monomials in $\mathcal{TL}$ are equal only if they are related by the relation (2.8). Since this lifts to an isomorphism $U_i \otimes U_j \cong U_j \otimes U_i$ in $\mathcal{TLC}_2$, we have $u_{\underline{\boldsymbol{i}}} = u_{\underline{\boldsymbol{j}}} \implies U_{\underline{\boldsymbol{i}}} \cong U_{\underline{\boldsymbol{j}}}$.

If an object has a 1-dimensional space of degree 0 endomorphisms, then it must be spanned by the identity map, and there can be no non-trivial idempotents. If an object has endomorphisms only in non-negative degrees, then it can not be isomorphic to any nonzero degree shift of itself. If two objects X and Y are such that both $\text{HOM}(X, Y)$ and $\text{HOM}(Y, X)$ are concentrated in strictly positive degrees, then no grading shift of X is isomorphic to Y, since there can not be a degree zero map in both directions.

Therefore, we will win if we show that $U_{\underline{\boldsymbol{i}}}$ has endomorphisms concentrated in non-negative degree, with a 1-dimensional degree 0 part, and that when $u_{\underline{\boldsymbol{i}}} \neq u_{\underline{\boldsymbol{j}}}$, $\text{HOM}(U_{\underline{\boldsymbol{i}}}, U_{\underline{\boldsymbol{j}}})$ is in strictly positive degrees. This question is entirely determined by the pairing on $\mathcal{TL}$, since it only asks about the graded dimension of Hom spaces.

When $\underline{\boldsymbol{i}}$ is empty, we already know that $(1, 1) = \frac{t^n}{(1-t^2)}[2]^n - \frac{t^2}{(1-t^2)}$, which has degree 0 coefficient 1, and is concentrated in non-negative degrees.

We know how to calculate $(x, y)_{\psi_0}$ in $\mathcal{TL}$ when x and y are monomials, and either x or y is not 1 (see Section 2.2). We draw x as a crossingless matching, draw y upside-down and place it below x, and close off the diagram: if there are m circles in the diagram, then $(x, y) = \frac{t^n[2]^{m-1}}{1-t^2}$. In particular, if $m = n + 1$ then the Hom space will be

concentrated in non-negative degrees, with 1-dimensional degree 0 part. If $m < n+1$ then the Hom space will be concentrated in strictly positive degrees.

We leave it as an exercise to show that, if x is a crossingless matching (i.e. a 321-avoiding monomial) then the closed diagram for (x, x) has exactly $n+1$ circles. The following example makes the statement fairly clear:

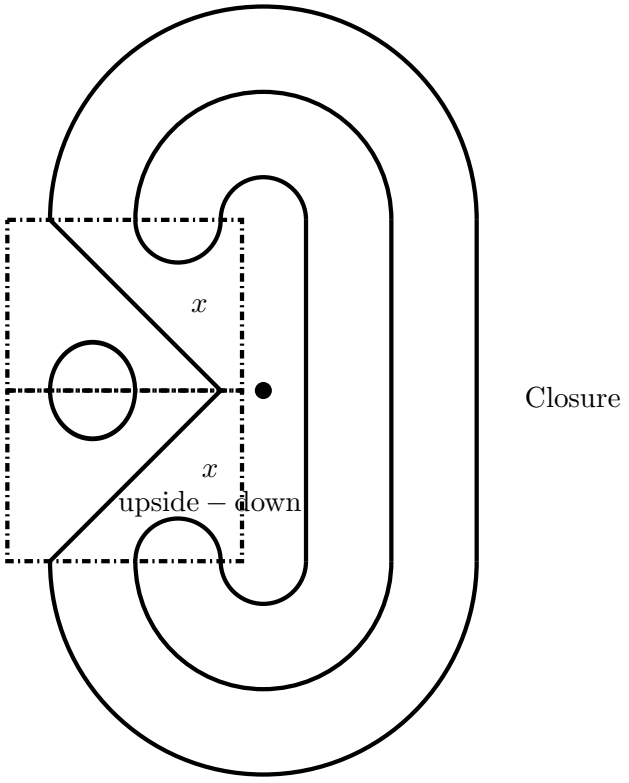

In this example x has all 3 kinds of arcs which appear in a crossingless matching: bottom to top, bottom to bottom, and top to top. Each of these corresponds to a single circle in the diagram closure.

Similarly, there are fewer than $n+1$ circles in the diagram for (x, y) whenever the crossingless matchings x, y are non-equal. Looking at the diagram above, keeping the upside-down x region but with the region x removed, one can see that no circles are yet completed, and each boundary point of x's region is matched to another by an arc. The number of circles is maximized when you pair these boundary points to each other, and this clearly gives the matching x. For any other matching y, two arcs will become joined into one, and fewer than $n+1$ circles will be created. □

Lemma 3.5. *$\mathcal{TLC}_2$ is idempotent-closed, and its indecomposables can all be expressed as grading shifts of $U_{\underline{\boldsymbol{i}}}$ for $\underline{\boldsymbol{i}}$ 321-avoiding. It has the Krull-Schmidt property.*

Proof. Since the Temperley-Lieb relations allow one to reduce a general word to a 321-avoiding word, one can show that every $U_{\underline{\boldsymbol{i}}}$ is isomorphic to a direct sum of shifts of $U_{\underline{\boldsymbol{j}}}$

for 321-avoiding $\underline{\boldsymbol{j}}$, using isomorphisms and direct sum decompositions instead of the analogous Temperley-Lieb relations. Clearly these shifted $U_{\underline{j}}$ are all indecomposable, since they have no non-trivial idempotents; these are then all the indecomposables. Since every indecomposable in $\mathcal{TLC}_2$ has a local endomorphism ring (with maximal ideal given by positively graded morphisms), $\mathcal{TLC}_2$ is idempotent-closed and has Krull-Schmidt. □

The Krull-Schmidt property implies that isomorphism classes of indecomposables form a basis for the Grothendieck group.

Proof of Main Theorem, given Lemma 3.3. There is a $\mathbb{Z}[t, t^{-1}]$-linear map of rings $\mathcal{TL} \to K(\mathcal{TLC}_2)$, which is evidently bijective because it sends the 321-avoiding basis to the 321-avoiding basis. Since $\mathcal{TLC} = \mathcal{TLC}_2$, we are done. □

Remark 3.6. In analogy to the paper [6], the bulk of the proof lies in proving that the Hom spaces in $\mathcal{TLC}_1$ obey some nice semi-linear form. Beyond that, in this paper, we mostly state the obvious.

However, some statements which are obvious in this paper are *not* obvious at all when dealing with $\mathcal{HC}$ and $\mathcal{H}$! Allow that we have already defined a category $\mathcal{HC}_1$ and shown that its Hom spaces induce the desired semi-linear product on $\mathcal{H}$. There is no simple way to conclude that $\mathcal{HC}$ categorifies $\mathcal{H}$, in analogy to the above. We summarize the differences here.

It is clear (for both Hecke and Temperley-Lieb) that the map $\mathcal{H} \to K(\mathcal{HC}_2)$ is well-defined and surjective. The two main subtleties are 1) the difference between $\mathcal{HC}_2$ and $\mathcal{HC}$, and 2) the injectivity of the map.

In general, one likes to examine the additive Grothendieck group only of idempotent-complete categories with the Krull-Schmidt property, because this guarantees that indecomposables form a basis for the Grothendieck group. However, taking the Karoubi envelope may increase the size of the Grothendieck group (for example, if M and N are non-isomorphic simples in a semisimple category, then the category generated by $M \oplus N$ has Grothendieck group $\mathbb{Z}$, while its idempotent closure has Grothendieck group $\mathbb{Z} \times \mathbb{Z}$). It is very convenient that $\mathcal{TLC}_2$ is already idempotent-closed, primarily because this implies that $\mathcal{TLC}_2$ and $\mathcal{TLC}$ have the same Grothendieck group. However, $\mathcal{HC}_2$ is not idempotent-closed, nor do we currently understand the idempotents. Thankfully, we have a result of Soergel [21]: each monomial $B_{\underline{\boldsymbol{i}}}$ has a (direct summand) filtration by indecomposables in $\mathcal{H}$, and an "upper triangular matrix" argument shows that the Grothendieck group is unchanged by passing to the Karoubi envelope.

To show injectivity of the map in the $\mathcal{TL}$ case, we can identify a basis of $\mathcal{TL}$ which is sent to a complete set of indecomposables, and then we can evaluate the trace map to show that these indecomposables are pairwise non-isomorphic. For $\mathcal{HC}$, we do not currently know what the indecomposables (i.e. idempotents) are, nor do we know what basis in $\mathcal{H}$ is their preimage. One hopes that the preimages of indecomposables are exactly the Kazhdan-Lusztig basis, but this is actually a deep question, shown by

Soergel ([22], see also [18, 21]) to be equivalent to proving a version of the Kazhdan-Lusztig conjectures. In any case, the result depends on the base field $\Bbbk$, and it has no simple proof. Not knowing the preimages (or conversely, not knowing a set of indecomposables which correspond to the Kazhdan-Lusztig basis), we may not calculate the Hom spaces by evaluating the trace map, and thus have no simple way of proving that these indecomposables are pairwise non-isomorphic. The proof of injectivity in the $\mathcal{HC}$ case used the fact that we can relate the diagrammatics to Soergel's previously constructed theory, for which Soergel's powerful geometric techniques can show that it categorifies the Hecke algebra (for certain $\Bbbk$). In particular, there is currently no proof of injectivity if one defines the category $\mathcal{HC}$ diagrammatically over $\Bbbk = \mathbb{Z}$.

It should be emphasized that the story of $\mathcal{TL}$ is a particularly easy one. No high-powered technical machinery is needed, and the proofs of idempotent closure and injectivity are self-contained and diagrammatic. In fact, the arguments in this paper *do* work entirely over $\mathbb{Z}[\frac{1}{2}]$, as can be checked. Dividing by two must be allowed in order to split the identity of U_{ii} into idempotents, as in (2.28); however, it is likely that the arguments would work over $\mathbb{Z}$ as well. Working over $\mathbb{Z}$ is discussed more extensively in [7].

3.3. **Reductions.** To show Lemma 3.3 we need only investigate the Hom spaces $\mathrm{HOM}(\emptyset, \underline{\boldsymbol{i}})$ for $\underline{\boldsymbol{i}}$ increasing, since we have already shown that the values of $\varepsilon(u_{\underline{\boldsymbol{i}}})$ are determined by their values for $\underline{\boldsymbol{i}}$ increasing. This space will be an R-bimodule where the left and right action are the same (since the lefthand and righthand regions are the same in any picture with no bottom boundary), so we view it as an R-module. We show in this section that this R-module is generated by a single element $\varphi_{\underline{\boldsymbol{i}}}$ as pictured here:

Let $I_{\underline{\boldsymbol{i}}}$ be the ideal which is the kernel of the map $R \to \mathrm{HOM}(\emptyset, \underline{\boldsymbol{i}})$ sending $1 \mapsto \varphi_{\underline{\boldsymbol{i}}}$; we call it the *TL ideal* of $\underline{\boldsymbol{i}}$. To prove the main lemma is to find $I_{\underline{\boldsymbol{i}}}$ and show that the graded dimension of $R/I_{\underline{\boldsymbol{i}}}$ is (up to a shift) $\psi_0(\underline{\boldsymbol{i}})$.

That $\varphi_{\underline{\boldsymbol{i}}}$ generates the Hom space is the conclusion of Corollary 2.4, the proof of which comprises the bulk of [6]. It is much easier to prove in $\mathcal{TLC}_1$ than in $\mathcal{HC}$, and since we will use the same arguments again, we reprove it for $\mathcal{TLC}_1$ below.

Effectively, we are just using the following rule to simplify cycles, which is an implication of the dot forcing rules and (2.13):

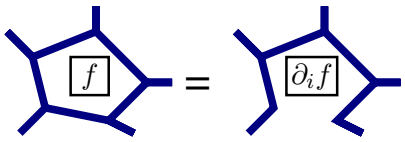

When we say that a graph or a morphism "reduces" to a set of other graphs, we mean that the morphism is in the $\Bbbk$-span of those graphs. We refer to a one-color graph, each of whose (connected) components is either a simple tree with respect to its boundary or a double dot, as a *simple forest with double dots*. If there are no double dots, it is a *simple forest without double dots*. Tree reduction implies that any graph without cycles

reduces to a simple forest with double dots. Note also that circles in a graph are equal to needles with a dot attached, and can be treated just like any other cycle.

Proposition 3.7. *In $\mathcal{TLC}_1$ any morphism reduces to one where, for each i, the i-graph is a simple forest with double dots. Moreover, we may assume all double dots are in the lefthand region.*

Proof. The dot forcing rules imply that double dots may be moved to any region of the (multicolored) graph, at the cost of breaking a few lines. Breaking lines will never increase the number of cycles. Therefore, if we have a graph without cycles, tree reduction implies that we actually have a simple forest with double dots, and dot forcing allows us to move these double dots to the left. The breaking of lines may require more tree reduction, yielding more double dots, but a simple induction (say, on the degree of the graph ignoring double dots on the left) will clearly suffice.

Now we induct on the number of cycles present in the overall graph. Suppose there is a blue colored cycle: choose one so that it delineates a single region (i.e. there are no other cycles inside). There may be blue "spokes" going from this cycle into the interior, but they must all be trees, lest they create another region. By tree reduction, we can assume that any blue appearing inside the cycle is in a different blue component than the cycle. Other colors may cross over the cycle, into the interior, but viewing the interior of the cycle as a graph of its own, then the boundary of the graph has no blue, and no colors adjacent to blue. The interior also has fewer total cycles, so using induction, we see that any blue or adjacent color inside the cycle reduces to double dots. The double dots can be slid out at the cost of potentially breaking an edge in the cycle, and the graph with the broken edge falls by induction. What remains is a blue cycle with no blue or any adjacent colors in the middle. But all distant colors can be slid out of the way, leaving an empty blue cycle, which is 0 by the rule above. □

Remark 3.8. This proposition and its proof will apply to graphs in any connected simply-connected region in the plane.

Remark 3.9. We want to find the TL ideal of $\underline{\boldsymbol{i}}$. Since the space $\mathrm{Hom}_{\mathcal{HC}_1}(\emptyset, \underline{\boldsymbol{i}})$ is a free R-module, all polynomials in $I_{\underline{\boldsymbol{i}}}$ must have arisen from reducing to some morphism which contained the relation (3.5) to a "nice form," i.e. $\varphi_{\underline{\boldsymbol{i}}}$ plus double dots. In other words, letting α_i be the morphism pictured below, we want to plug α_i into a bigger graph, reduce it to a nice form, and see what we get.

This bigger graph, into which α_i is plugged, will actually be a graph on the *punctured plane* or *punctured disk* with specified boundary conditions on both the outer and inner boundary. The difficult graphical proofs of this paper just consist in analyzing such graphs. This is done by splitting the punctured plane into simply-connected regions, and using the above proposition.

Remember that α_i is just a 6-valent vertex with two dots attached (one red and one blue).

3.4. **Generators of the TL Ideal.** The sequence $\underline{\boldsymbol{i}}$ is assumed to be non-repeating.

Proposition 3.10. *The TL ideal of $\emptyset$ contains $y_{i,j} \stackrel{def}{=} f_i f_j(f_i + 2f_{i+1} + 2f_{i+2} + \ldots + 2f_{j-1} + f_j)$ over all $1 \leq i < j \leq n$.*

The TL ideal of $\underline{\boldsymbol{i}}$ contains $z_{i,j,\underline{\boldsymbol{i}}} \stackrel{def}{=} \frac{y_{i,j}}{g_i g_j}$ where $g_i = f_i$ if $i \in \underline{\boldsymbol{i}}$, $g_i = 1$ otherwise.

We will prove that these actually generate the ideal in Proposition 3.28.

Proof. Adding 4 dots to α_i, or 6 dots to a 6-valent vertex, we get

(3.11)  .

This is $y_{i,i+1} = f_i f_{i+1}(f_i + f_{i+1}) = (x_i - x_{i+1})(x_{i+1} - x_{i+2})(x_i - x_{i+2})$ (which cuts out 3 Weyl walls in V).

Even though we are not allowing 6-valent vertices in our diagrams, we will sometimes express $y_{i,i+1}$ as

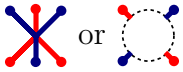

to avoid having to consider sums of graphs (it's easier for me to draw!).

To obtain the other $y_{i,j}$, note the following equalties under the action of S_{n+1} on R:

$$s_i f_{i+1} = f_i + f_{i+1} \tag{3.12}$$
$$s_{i+1} f_i = f_i + f_{i+1} \tag{3.13}$$
$$s_i f_i = -f_i \tag{3.14}$$
$$s_i f_j = f_j \text{ for } |i-j| > 1 \tag{3.15}$$

From this it follows by explicit calculation that

$$s_{i-1} y_{i,j} - y_{i,j} = y_{i-1,j} \tag{3.16}$$
$$s_{j+1} y_{i,j} - y_{i,j} = y_{i,j+1} \tag{3.17}$$

Now, when we surround a polynomial f with a j-colored circle, we get $f - s_j f = \partial_j(f) f_j$.

(3.18) 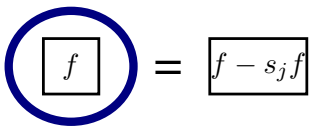

Hence, a $k+2$ circle around $y_{k,k+1}$ will yield $y_{k,k+2}$ (up to a sign), etcetera. We have numerous ways to express $\pm y_{i,j}$: for any $i \leq k \leq j-1$ take α_k with 4 dots to get $y_{k,k+1}$, and then surround it with concentric circles whose colors, from inside to out, are $k+2, k+3, \ldots, j$ and then $k-1, k-2, \ldots, i$.

Clearly the colors of the increasing sequence and those of the decreasing sequence are distant, so a sequence like $k-1, k+2, k+3, k-2, \ldots$ is also ok, or any permutation which preserves the order of the increasing and the decreasing sequence individually.

For very similar reasons, $z_{i,j,\underline{\boldsymbol{i}}}$ is in the TL ideal of $\underline{\boldsymbol{i}}$. Adding two or three dots to (3.5), we get several more equations.

(3.19)

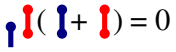

(3.20)

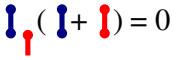

(3.21)

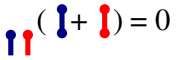

Again, for various of these pictures we use shorthand like

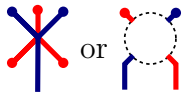

These give you $z_{i,i+1,\underline{\boldsymbol{i}}}$ in the case where at least one of $i, i+1 \in \underline{\boldsymbol{i}}$. Putting a polynomial f in the eye of a j-colored needle will yield $\partial_j(f) = \frac{f - s_j f}{f_j}$ next to a j-colored boundary dot.

(3.22)

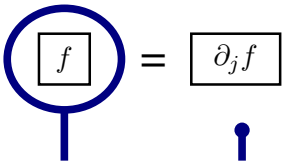

This gives us several ways to draw $z_{i,j,\underline{\boldsymbol{i}}}$.

If neither i nor j are in $\underline{\boldsymbol{i}}$, then $z_{i,j,\underline{\boldsymbol{i}}} = y_{i,j}$ and is pictured as above, but with additional boundary dots put below to account for $\varphi_{\underline{\boldsymbol{i}}}$. Since these extra dots are generally irrelevant, we often do not bother to draw them.

If $i \in \underline{\boldsymbol{i}}$ and $j \notin \underline{\boldsymbol{i}}$, we have two ways of drawing $z_{i,j,\underline{\boldsymbol{i}}}$. One can take α_i, connect one i input to the outer boundary, add dots, and surround it with circles colored $i+2, i+3, \ldots, j$.

(3.23)

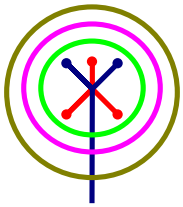

Alternatively, take some $i < k < j$, add dots to α_k, and surround it with circles forming an increasing sequence $k+2 \dots j$ and a decreasing sequence $k-1 \dots i$, *except* that the final i-colored circle is a needle.

(3.24)

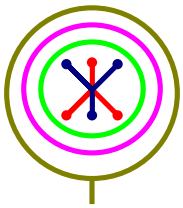

The case of $j \in \underline{\boldsymbol{i}}$ and $i \notin \underline{\boldsymbol{i}}$ is obvious.
If both $i, j \in \underline{\boldsymbol{i}}$ then we have several choices again. If $j = i+1$ then we must use

(3.25)

but in general we may either repeat (3.23) with a j-needle instead of a j-circle

(3.26)

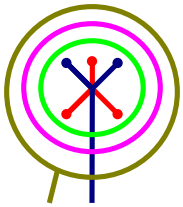

or repeat (3.24) with a j-needle instead of a j-circle.

(3.27)

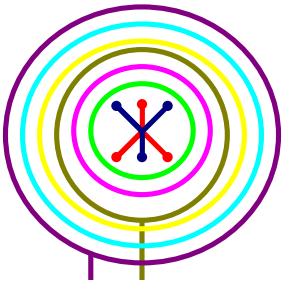

In any case, it is clear that the polynomials above are in the TL ideal, and the claim is proven. □

Let us quickly consider the redundancy in this generating set of the ideal. When $i > j$ let $y_{i,j} \stackrel{\text{def}}{=} y_{j,i}$ and $z_{i,j,\underline{\boldsymbol{i}}} \stackrel{\text{def}}{=} z_{j,i,\underline{\boldsymbol{i}}}$.

Corollary 3.11. *Suppose $\underline{\boldsymbol{i}}$ is non-empty, and fix an index $k \in \underline{\boldsymbol{i}}$. Then $I_{\underline{\boldsymbol{i}}}$ is generated by $z_{k,j,\underline{\boldsymbol{i}}}$ for $1 \leq j \leq n$, $j \neq k$. None of these generators is redundant.*

None of the generators $y_{i,j}$ of $I_\emptyset$ are redundant.

Proof. We leave the checks of irredundancy to the reader, but a proof will also arise as a byproduct in the next section.

Suppose that $k \in \underline{\boldsymbol{i}}$ but $i, j \notin \underline{\boldsymbol{i}}$ do not. If $k < i < j$, then $z_{i,j,\underline{\boldsymbol{i}}} = y_{i,j} = f_i z_{k,j,\underline{\boldsymbol{i}}} - f_j z_{k,i,\underline{\boldsymbol{i}}}$ so that $z_{i,j,\underline{\boldsymbol{i}}}$ is redundant. If $i < k < j$, then $z_{i,j,\underline{\boldsymbol{i}}} = f_i z_{k,j,\underline{\boldsymbol{i}}} + f_j z_{i,k,\underline{\boldsymbol{i}}}$. A similar statement holds for $i < j < k$. In the same vein, if $k, l \in \underline{\boldsymbol{i}}$ but $i \notin \underline{\boldsymbol{i}}$, then given $z_{k,l,\underline{\boldsymbol{i}}}$ only one of $z_{k,i,\underline{\boldsymbol{i}}}$ or $z_{l,i,\underline{\boldsymbol{i}}}$ is needed, and if $k, l, m \in \underline{\boldsymbol{i}}$, then any 2 of the three pairwise relations will imply the third. □

3.5. **Graded Dimensions.** In this section, fix a non-repeating sequence $\underline{\boldsymbol{i}}$. We assume that the generators of $I_{\underline{\boldsymbol{i}}}$ are precisely the polynomials described in Proposition 3.10.

Notation 3.12. An element of R can be written as a polynomial in f_i, so let $x = f_1^{a_1} \dots f_n^{a_n}$ be a general monomial. Choose any $\underline{\boldsymbol{i}}$, possibly empty. Given a monomial x, let $J_x \subset \{1, \dots, n\}$ be the subset containing $\underline{\boldsymbol{i}}$ and all indices j such that $a_j \neq 0$. For a fixed subset J, let R_J be the subset of all monomials x with $J_x = J$. This inherently depends on the choice of $\underline{\boldsymbol{i}}$.

Under the map $R \to \mathrm{HOM}(U_\emptyset, U_{\underline{\boldsymbol{i}}})$, the image of R_J will be graphs where the colors appearing are precisely J. Every color in $\underline{\boldsymbol{i}}$ appears as a boundary dot, and every f_j corresponds to a double dot of that color. The case $J = \emptyset$ only occurs when $\underline{\boldsymbol{i}} = \emptyset$, and $R_\emptyset = \{1\}$.

We rewrite the generating polynomials of $I_{\underline{\boldsymbol{i}}}$ in a suggestive form, in order to apply the Bergman Diamond Lemma [1].

Let us consider $\underline{\boldsymbol{i}} = \emptyset$. The equation $y_{i,j} = 0$ for $i < j$ is equivalent to $f_i f_j^2 = -(f_i^2 f_j + \sum_{i<k<j} 2 f_i f_j f_k)$. Putting the lexicographic order on monomials, this replaces $f_i f_j^2$ with a sum of monomials all lower in the order. We view this relation as a way to lower the order, and we only apply it to replace the LHS with the RHS and not vice versa. A monomial is *irreducible* if no relations $y_{i,j} = 0$ can be used to lower the order, which is equivalent to the statement that $f_i f_j^2$ never appears as a factor for any $i < j$.

Claim 3.13. *Let $\underline{\boldsymbol{i}} = \emptyset$. For each $J \neq \emptyset$, the irreducible monomials in R_J are precisely $f_k^m \prod_{i \in J} f_i$, where k is the minimal index in J and $m \geq 0$ (note: the exponent of f_k is $m + 1 \geq 1$). When $J = \emptyset$, 1 is irreducible.*

Proof. This is obvious. □

Claim 3.14. *Let $\underline{\boldsymbol{i}} = \emptyset$. Then irreducible monomials form a basis for $R/I_\emptyset$.*

Proof. That they span is clear. That they are independent is a result of the Bergman Diamond Lemma [1]. Quickly: when monomials are given a partial order which is

bounded below, relations are given in order-lowering format, and certain coherence conditions hold, then the Diamond Lemma implies that irreducibles form a basis for the quotient. The coherence conditions state that for the simplest possible ambiguities (monomials where one could reduce them in two different ways), both ways of reducing them will reduce further to the same value. The relevant ambiguities are $(i < l < j)$ $f_i f_l f_j^2$, where one can resolve either factor $f_i f_j^2$ or $f_l f_j^2$, and $f_i f_l^2 f_j^2$, where one can resolve either factor $f_i f_l^2$ or $f_l f_j^2$. It is a trivial exercise to check the coherence conditions. $\square$

Remark 3.15. This also proves that none of the $y_{i,j}$ is redundant. If one were redundant, then one should get the same basis of irreducibles without that particular reduction move, but clearly $f_i f_j^2$ is irreducible without the appropriate reduction move.

When $J \neq \emptyset$, the graded rank of the irreducibles in R_J is $\frac{t^{2|J|}}{1-t^2}$. When J is empty, the only element of R_J is 1. So the graded rank of $R/I_\emptyset$ is $1 + \sum_{J \neq \emptyset} \frac{t^{2|J|}}{1-t^2}$. But $\sum_J t^{2|J|} = (1+t^2)^n$ since every f_i may either appear or not appear, independently of every other. Hence $\sum_{J \neq \emptyset} t^{2|J|} = (1+t^2)^n - 1$. Putting it all together, the graded rank is $\frac{(1+t^2)^n - t^2}{1-t^2} = \frac{t^n[2]^n - t^2}{1-t^2}$. Hence we have proven

Claim 3.16. *The graded dimension of $R/I_\emptyset\{d\}$ is exactly $\psi_0(\emptyset)$.*

Now consider $\underline{\boldsymbol{i}} \neq \emptyset$, and fix $k \in \underline{\boldsymbol{i}}$. We choose a different order on indices, where $k < k+1 < k-1 < k+2 < k-2 < \ldots$, and then place the lexicographic order on monomials. We rewrite $z_{k,j,\underline{\boldsymbol{i}}}$ for $j \neq k$ in order-decreasing format as either $f_j^2 = -(f_k f_j + \sum_l 2 f_l f_j)$ for $j \notin \underline{\boldsymbol{i}}$, or $f_j = -(f_k + \sum_l 2 f_l)$ for $j \in \underline{\boldsymbol{i}}$, where the sum is over l between k and j. An *irreducible* polynomial will then be a polynomial which does not have f_j^2 as a factor, for $k \neq j \notin \underline{\boldsymbol{i}}$, and does not have f_j as a factor for $k \neq j \in \underline{\boldsymbol{i}}$.

Claim 3.17. *Let $\underline{\boldsymbol{i}} \neq \emptyset$ and fix $k \in \underline{\boldsymbol{i}}$. The irreducible monomials in R_J are precisely $f_k^m \prod_{j \in J \setminus \underline{\boldsymbol{i}}} f_j$ for $m \geq 0$.*

Claim 3.18. *Irreducibles form a basis for $R/I_{\underline{\boldsymbol{i}}}$.*

Proof. The first claim is obvious, and the second follows from the Diamond Lemma. We leave this as an exercise. $\square$

The graded rank of irreducibles in R_J is $\frac{t^{2|J|-2d}}{1-t^2}$, for d the length of $\underline{\boldsymbol{i}}$ (remember that $\underline{\boldsymbol{i}} \subset J$). Thus the graded rank of $R/I_{\underline{\boldsymbol{i}}}$ is $\sum_{\underline{\boldsymbol{i}} \subset J} \frac{t^{2|J|-2d}}{1-t^2} = \frac{(1+t^2)^{n-d}}{1-t^2}$, and the graded rank of $R/I_{\underline{\boldsymbol{i}}}\{d\}$ is $t^d \frac{(1+t^2)^{n-d}}{1-t^2} = \frac{t^n[2]^{n-d}}{1-t^2}$. Hence,

Claim 3.19. *The graded dimension of $R/I_{\underline{\boldsymbol{i}}}$ is exactly $\psi_0(\underline{\boldsymbol{i}})$.*

This is clearly sufficient to prove Lemma 3.3.

3.6. **Weyl Lines.** We continue to assume that $\underline{\boldsymbol{i}}$ is non-repeating and $z_{i,j,\underline{\boldsymbol{i}}}$ generates $I_{\underline{\boldsymbol{i}}}$.

Definition 3.20. Let V be the geometric representation of S_{n+1}, such that $R = \mathbb{C}[f_1, \ldots, f_n]$ is the coordinate ring of V. Note that the linear equations which cut out reflection-fixed hyperplanes are precisely $w_{i,j} = f_i + f_{i+1} + \ldots + f_j = x_i - x_{j+1}$ for $i \leq j$. A *Weyl line* is a line in V through the origin which is defined by the intersection of reflection-fixed hyperplanes; it is given by a choice of $n-1$ transversely-intersecting reflection-fixed hyperplanes. Given a non-repeating sequence $\underline{\boldsymbol{i}}$, we say a Weyl line is *transverse to* $\underline{\boldsymbol{i}}$ if it is transverse to (i.e. not contained in) the hyperplanes $f_k = 0$ for each $k \in \underline{\boldsymbol{i}}$.

Proposition 3.21. *The TL ideal of $\underline{\boldsymbol{i}}$ is the ideal associated with the union of all Weyl lines transverse to $\underline{\boldsymbol{i}}$ (with its reduced scheme structure).*

Proof. The proof is simple, and we sketch it here. Use induction on the number of colors n ($n = 1, 2$ is obvious).

For any $1 \leq k \leq n$, consider the hyperplane $f_k = 0$ as an $n-1$-dimensional space, with an action of S_n (essentially, just pretend the index k didn't exist). It is easy to check that the non-zero images of $w_{i,j}$ now cut out exactly the Weyl lines of $f_k = 0$, and that the non-zero images of $y_{i,j}$ are the equivalent polynomials $y_{i,j}$ for that smaller root system. Therefore, by induction, the vanishing set of $y_{i,j}$ agrees with the Weyl lines on $f_k = 0$.

If all $f_k \neq 0$, then it is easy to check that both $y_{i,j}$ and $w_{i,j}$ cut out a single line, namely $-f_1 = f_2 = -f_3 = \ldots = (-1)^n f_n$. So $I_\emptyset$ cuts out precisely the Weyl lines.

For $\underline{\boldsymbol{i}} \neq \emptyset$, the vanishing of $I_{\underline{\boldsymbol{i}}}$ is contained in that of $I_\emptyset$. Choose $k \in \underline{\boldsymbol{i}}$. If $f_k = 0$ then $z_{k,k+1,\underline{\boldsymbol{i}}}$ is equal to f_{k+1}^a where $a = 1, 2$ depending on whether $k+1 \in \underline{\boldsymbol{i}}$, but either way we get that $f_{k+1} = 0$. Then $z_{k,k+2} = f_{k+2}^a$ for $a = 1, 2$, and so forth. Therefore $f_k = 0$ only intersects the vanishing of $I_{\underline{\boldsymbol{i}}}$ at the origin. It is clear that, on the open set where $f_k \neq 0$ for all $k \in \underline{\boldsymbol{i}}$, the polynomials $z_{i,j,\underline{\boldsymbol{i}}}$ and $y_{i,j}$ have the same vanishing, since they differ by a unit. □

Remark 3.22. It is also easy to show by induction that the ideal $I_{\underline{\boldsymbol{i}}}$ actually gives the induced reduced scheme structure on that union of Weyl lines.

Remark 3.23. In particular, $I_\emptyset$ is contained in every ideal, and the quotient category $\mathcal{TLC}_1$ is manifestly $R/I_\emptyset$-linear.

Remark 3.24. Let Z be the union of all Weyl lines in V. The previous results should lead one to guess that the Temperley-Lieb algebra should be connected to the geometry of the S_{n+1} action on Z via $\mathcal{TLC}$, in much the same way that the Hecke algebra is connected to the geometric representation via $\mathcal{HC}$ (see the introduction). However, we have not succeeded in formulating the category $\mathcal{TLC}$ in terms of coherent sheaves on $Z \times Z$, or equivalently as $R/I_\emptyset$-bimodules. It is no longer true that Hom spaces are free left modules, and this makes homological algebra difficult. Our attempts to describe what happens when you "pull back" the category $\mathcal{HC}_1$ along the closed immersion from Z to V have also not met with any success. Describing $\mathcal{TLC}$ using sheaves on Z seems like an interesting question.

As an example of the difficulties, let U_i be the bimodule $R/I_i \otimes R/I_i\{-1\}$, where the tensor is over R^{s_i}; this should be the equivalent of the Soergel bimodule B_i. The maps below are given their usual Frobenius algebra names. Then there is a degree 1 map $R/I_\emptyset \to U_i$ sending 1 to $x_i \otimes 1 - 1 \otimes x_{i+1}$ (the unit), but there is no degree 1 map $U_i \to R/I_\emptyset$ corresponding to the counit (it should send $1 \otimes 1$ to 1). There is only a degree 3 map, sending $1 \otimes 1$ to f_i. A similar problem occurs again: comultiplication is well-defined in the naive sense, but multiplication is not unless you throw in a factor of f_i in the appropriate place.

Now we describe briefly the topological intuition associated with the category $\mathcal{TLC}$, and another way to view $I_{\underline{\boldsymbol{i}}}$. These remarks will not be used in the remainder of the paper. The reader should be acquainted with the section on $\mathfrak{sl}_2$-foams in Vaz's paper [25].

Remark 3.25. Let $\mathcal{F}$ be the functor from $\mathcal{TLC}_1$ to the category of disoriented cobordisms Foam_2, as defined in Vaz's paper. If f_i is the double dot colored i, then one can easily see that $\mathcal{F}$ sends f_i to a tube connecting the ith sheet to the $(i+1)$th sheet, with a disorientation on it. If the double dot appears in a larger morphism φ, such that in $\mathcal{F}(\varphi)$ the ith sheet and the $(i+1)$th sheet are already connected by a saddle or tube, then adding another tube between them does nothing more than add a disoriented handle to the existing surface.

Suppose that the ith, $(i+1)$th, and $(i+2)$th sheets are all connected in a cobordism. Then f_i adds a handle on the left side of the $(i+1)$th sheet, f_{i+1} adds a handle on the right side, and these two disoriented surfaces are equal up to a minus sign in Foam_2. This fact is essentially the statement that:

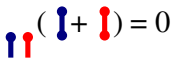

In other words, the algebra $\Bbbk[f_1, \ldots, f_n]$ acts on cobordisms of $n+1$ sheets, where f_i places a tube between the ith and $(i+1)$th sheet. The ideal $I_{\underline{\boldsymbol{i}}}$ is clearly in the kernel of this action when applied to the cobordism $\mathcal{F}(\varphi_{\underline{\boldsymbol{i}}})$.

Remark 3.26. It seems to the author that it should be easy to show that $I_{\underline{\boldsymbol{i}}}$ is precisely the kernel of the above action, or equivalently that $R/I_{\underline{\boldsymbol{i}}}$ (with dots $\underline{\boldsymbol{i}}$ below) is sent injectively by $\mathcal{F}$ to Foam_2. This would be entirely sufficient to show that the functor $\mathcal{F}$ is faithful. To prove this, equip $\mathcal{TL}$ with a semi-linear product given by Hom spaces in the image of $\mathcal{F}$, i.e. $([M],[N]) = \mathrm{grk}\,\mathcal{F}(\mathrm{HOM}_{\mathcal{TLC}_1}(M,N))$ for any objects M, N in $\mathcal{TLC}$. For the usual reasons this is a well-defined semi-linear product, and has an associated a trace map. Checking faithfulness of $\mathcal{F}$ on $\mathrm{HOM}(\emptyset, \underline{\boldsymbol{i}})$ for $\underline{\boldsymbol{i}}$ increasing will show that this trace is equal to the usual trace on $\mathcal{TL}$, and thus that the functor must be faithful on every Hom space.

Remark 3.27. If one can show that $z_{i,j,\underline{\boldsymbol{i}}}$ generate the kernel of the above action, then this actually implies already that $z_{i,j,\underline{\boldsymbol{i}}}$ generate $I_{\underline{\boldsymbol{i}}}$, since the image of $\mathrm{HOM}_{\mathcal{TLC}_1}(\emptyset, \underline{\boldsymbol{i}})$ in Foam_2 must be a quotient of $R/I_{\underline{\boldsymbol{i}}}$. However, we will prove this fact diagrammatically as well.

3.7. **Proof of Generation.**

Proposition 3.28. *The TL ideal $I_\emptyset$ is generated by $y_{i,j} \stackrel{def}{=} f_i f_j (f_i + 2f_{i+1} + 2f_{i+2} + \ldots + 2f_{j-1} + f_j)$ over all $1 \leq i < j \leq n$.*

The TL ideal $I_{\underline{\boldsymbol{i}}}$ is generated by all $z_{i,j,\underline{\boldsymbol{i}}} \stackrel{def}{=} \frac{y_{i,j}}{g_i g_j}$ where $g_i = f_i$ if $i \in \underline{\boldsymbol{i}}$, $g_i = 1$ otherwise.

We wish to determine the ideal generated by α_k inside $\mathrm{HOM}(\emptyset, \underline{\boldsymbol{i}})$, for $\underline{\boldsymbol{i}}$ non-repeating. As discussed in Remark 3.9, our goal is to take any graph Γ on the punctured plane, with $\underline{\boldsymbol{i}}$ as its outer boundary and $k(k+1)k(k+1)$ as its inner boundary, plug α_k into the puncture, and reduce it to something in the ideal generated by the pictures of Section 3.4.

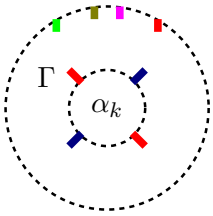

Our coloring conventions for this chapter will be that blue always represents the index k, red represents $k+1$, and other colors tend to be arbitrary (often, the number of other colors appearing is also arbitrary). However, it will often happen that colors will appear in increasing or decreasing sequences, and these will be annotated as such. Note that blue or red may appear in the outer boundary as well, but at most once each.

Let us study Γ, and not bother to plug in α_k. The only properties of α_k which we need are the following:

(3.28)

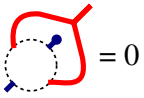

This follows from (3.1), or just from isotopy. The same holds with colors switched.

(3.29)

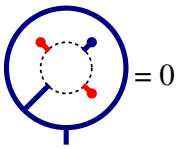

This is because the diagram reduces to a k-colored needle, with $f = f_{k+1}(f_k + f_{k+1})$ inside. But f is fixed by s_k, so it slides out of the needle, and the empty needle is equal to 0. A similar equality holds with colors switched.

(3.30)

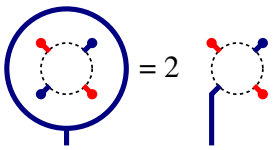

This follows from the above and the dot forcing rules.

The final property we use is that any graph only using colors $< k-1$ or $> k+2$ can slide freely across the puncture.

Note however that, say, an arbitrary $k-3$ edge can not automatically slide across the puncture, because a $k-2$ edge might be in the way, and this could be in turn obstructed by a $k-1$ edge, which can not slide across the blue at all.

The one-color reduction results apply to any simply-connected planar region, so we may assume (without even using the relation (3.5)) that in a simply connected region of our choice, the i-graph for each i is a simple forest with double dots. Any connected component of an i-graph that does not encircle the puncture will be contained in a simply-connected region, and hence can be simplified; this will be the crux of the proof. The proof is simple, but has many cases.

Remark 3.29. We will still need to use relation (3.5) as we simplify graphs.

We will treat cases based on the "connectivity" of Γ, that is, how many of the blue and red boundaries in the inner and outer puncture are connected with each other. We will rarely perform an operation which makes the graph more connected. At each stage, we will reduce the graph to something known to be in the ideal, or break edges to decrease the connectivity. We call an edge coming from the puncture an *interior line* and one coming from the outer boundary an *exterior line*.

Note also that any double dots that we can move to the exterior of the diagram become irrelevant, since the picture with those double dots is in the ideal generated by the picture without double dots. Also, any exterior boundary dots are irrelevant, since they are merely part of the map $\varphi_{\underline{i}}$ and do not interfere with the rest of the diagram at all.

Step 1: Suppose that the two interior red lines are in the same $k+1$-component of Γ. Then there is some innermost red path from one to the other, such that the interior of this path (the region towards the puncture) is simply-connected. Applying reductions, we may assume that the k-graph in this region consists of a blue boundary dot with double dots, and the $k+1$-graph and $k+2$-graph each consist only of double dots. We may assume all double dots occur right next to one of the red lines coming from the puncture. The current picture is exactly like that in (3.28), except that there may be double dots inside, and other colors may be present (also, there could be more red spokes emanating from the red arc, but these can be ignored or eliminated using (2.11) and tree reduction). However, the double dots may be forced out of the red enclosure at the cost of potentially breaking the red edge, and breaking it will cause the two red interior lines to be no longer in the same connected component. If there are no double dots, then all the remaining colors (which are $< k-2$ or $> k+1$) may be slid across the red line and out of the picture. Hence we are left with the exact picture of (3.28), which is zero.

Thus we may assume that the two red lines coming from the puncture are not in the same component. The same holds for the blue lines.

Step 2: Suppose that the component of one of the interior blue lines wraps the puncture, creating an internal region (which contains the puncture). Again, reducing in that internal region, the other interior blue line can not connect to the boundary so it must reduce to a boundary dot (with double dots), the reds may not connect to each other so each reduces to a boundary dot, and as before we are left in the picture of (3.29) except possibly with double dots and other colors. If there are no double dots, all other colors may be slid out, and the picture is zero by (3.29). Again, we can put the double dots near the exterior, and forcing them out will break the blue arc. It is still possible that some other cycle still allows that component to wrap the puncture; however, this process need only be iterated a finite number of times, and finitely many arcs broken, until that component no longer wraps the puncture.

So we may assume that the component of any interior line, red or blue, does not wrap the puncture. That component is contained in a simply-connected region, so it reduces to a simple tree. Hence, we may assume that the components of interior lines either end immediately in boundary dots, or connect directly to an external line of the same color (at most one such exists of each color).

Step 3: Suppose that there is a blue edge connecting an internal line directly to an external one. Consider the region Γ':

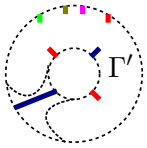

Then Γ' is simply-connected. Other colors in Γ may leave Γ' to cross through the blue line; however, the colors $k-1, k, k+1$ may not. Therefore, reducing within Γ', we may end the internal blue line in a boundary dot and eliminate all other instances of the color blue (since they become irrelevant double dots on the exterior), reduce red to a simple forest where the two interior lines are not connected (again, ignoring irrelevant double dots), and reduce $k-1$ to either the empty diagram or an external boundary dot (depending on whether $k+1 \in \underline{\boldsymbol{i}}$). Once this has been accomplished, the absence of the color $k-1$ implies that we may slide $k-2$ freely across the puncture! The color $k-2$ can be dealt with in the entire disk, which is simply connected, so it reduces to the empty diagram or an external boundary dot (depending on whether $k+2 \in \underline{\boldsymbol{i}}$). Then we may deal with color $k-3$, and so forth.

Thus, the existence of the blue edge implies that all colors $< k$ can be ignored: they appear in irrelevant double dots, in irrelevant boundary dots, or not at all. Similarly, the existence of a red edge allows us to ignore all colors $> k+1$.

Step 4: Let us only consider components of graphs which do not meet the internal boundary.

Lemma 3.30. *Consider a component of a graph on a punctured disk, which does not meet the internal boundary, and which meets the external boundary at most once. Then it can be reduced to one of the following, with double dots on the exterior: the empty*

graph; a boundary dot; a circle around the puncture; a needle coming from the external boundary, with its eye around the puncture.

Proof. Suppose that the component splits the punctured plane into m regions. If the component is contained in a simply-connected part of the punctured plane, we are done. This is always true for $m = 1$. So we may suppose that $m \geq 2$ and we have two distinguished regions: the external region, and the region containing the puncture. Any other region is one of two kinds, as illustrated in the following equality (due to (2.11):

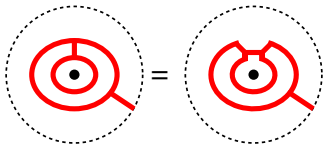

On the right side we have a region which is contained in a simply-connected part, and thus can be eliminated by reduction (see Proposition 3.7). On the left side the region is not contained in a simply-connected part, nor does it contain the puncture. However, any such region can be altered, using (2.11) as in the heuristic example above, into a cycle of the first kind. Therefore, we may assume there are exactly 2 regions.

In the event that there are two regions, we have a cycle which surrounds around the puncture, and may have numerous branches into both regions, internal and external. However, each branch must be a tree lest another region be created. These trees reduce in the usual fashion, and therefore the internal branches disappear, and the external branches either disappear or connect directly to the single exterior boundary. Thus we have either a needle or a circle. Double dots, as usual, can be forced out of the way possibly at the cost of breaking the cycle, and reducing to the case $m = 1$. □

Let us now examine the remaining cases. We shall ignore all parts of a graph which are double dots on the exterior, or are external boundary dots.

Case 1: Both a blue edge and a red edge connect an internal line to an external line. Then, as in Step 3, all other colors can be ignored, and the entire graph is

This, as explained in Section 3.4, is $z_{k,k+1,\underline{i}}$.

Case 2: A blue edge connects an internal line to an external line, and both red internal lines end in boundary dots. As discussed in Step 3, we may ignore all colors $< k$, and both colors k and $k+1$ do not appear in a relevant fashion outside of what is already described. We may ignore the presence of any double dots. However, there may be numerous circles and needles colored $\geq k+2$ which surround the puncture and cross through the blue line, in an arbitrary order.

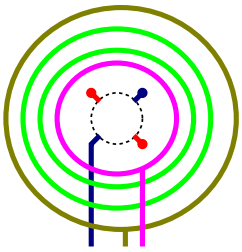

Claim 3.31. *The sequence of circles and needles can be assumed to form an increasing sequence of colors, from $k+2, k+3, \ldots$ until the final color, and that only the final color may be a needle.*

Proof. If the innermost circle/needle is not colored $k+2$, then it may slide through the puncture, and will evaluate to zero by (2.13). So suppose the innermost is $k+2$. If it is a needle, not a circle, then there can be no more $k+2$-colored circles, and no $k+3$-colored circles. Color $k+4$ can be pulled through the middle so resolved on the entire disk, and hence can be ignored, and so too with $k+5$ and higher. This is the "needle" analogy to the conclusion of Step 3: the existence of a m-colored needle around the puncture and the lack of m or $m+1$ on the interior of the needle will allow us to ignore all colors $\geq m+1$.

So suppose it is a $k+2$-colored circle. If the next circle/needle is colored $\geq k+4$ then it slides through the $k+2$ circle and the puncture, and evaluates to zero. If the next circle/needle is *also* colored $k+2$, then we may use the following calculation to ignore it. The calculation begins by using (2.28).

(3.31)

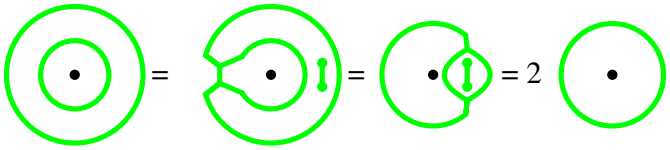

Thus we may assume that the next circle/needle is colored $k+3$. Again, if it is a needle, then we can ignore all other colors, and our picture is complete.

Similarly, the next circle/needle can not be colored $\geq k+5$ lest it slide through, and it can not be colored $k+3$ lest we use (3.31). If it is colored $k+2$, then we may use the following calculation to ignore it. The calculation begins by using (3.5), and assumes green and purple are adjacent.

(3.32)

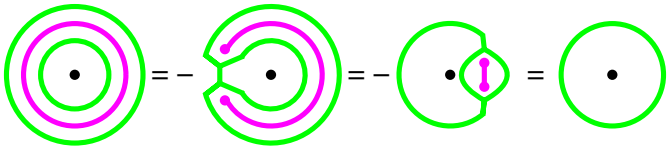

Thus we can assume the next circle/needle is colored $k+4$. If it is a needle, then all colors $k+5$ and higher can be ignored. Additional circles of color $k+2$ could run

through the needle, but these could be slid inwards and reduced as before. So if it is a needle, our picture is complete.

Finally, the next circle/needle can not be colored $\geq k+6$ lest it slide, $k+4$ lest we use (3.31), $k+3$ lest we use (3.32), or $k+2$ lest we slide it inside and reduce it as above. Hence it is colored $k+5$, and if it is a needle, we are done. This argument can now be repeated for the win. □

Thus our final picture yields $z_{k,j,\underline{i}}$ as in (3.23) or (3.26).

Note that the case of a red edge works the same way, with a decreasing sequence instead of an increasing sequence.

Case 3: All the internal lines end in boundary dots. We may assume that the remainder of the graph consists in circles/needles around this diagram, but have no restrictions at the moment on which colors may appear.

Claim 3.32. *We may assume that the colors in circles/needles form an increasing sequence from $k+2$ up, and a decreasing sequence from $k-1$ down (these sequences do not interact, so w.l.o.g. we may assume the increasing sequence comes first, then the decreasing one). Only the highest and lowest color may be a needle.*

Proof. The method of proof will be the same as the arguments of the previous case.

Consider the innermost circle/needle. If it is colored k or $k+1$, then we may use (3.30) to reduce the situation to a previous case. If it is colored $\geq k+3$ or $\leq k-2$ then it slides through the puncture. So we may assume it is $k+2$ or $k-1$. If it is a $k+2$-colored (resp. $k-1$-colored) needle, then the usual arguments imply that all colors $> k+2$ (resp. $< k-1$) can be ignored. This same argument with needles will always work, so we will not discuss the circle/needle question again, and speak as though everything is a circle.

Assume that the first colors appearing are an increasing sequence from $k+2$ to i and then a decreasing sequence from $k-1$ to j. Note that either sequence may be empty. If the next color appearing is $\leq j-2$ then it slides through the whole diagram and the puncture, and evaluates to zero. If the decreasing sequence is non-empty and the next color is j then we use (3.31); if it is $\geq j+1$ and $\leq k-1$ then we slide it as far in as it will go and use (3.32). If the decreasing sequence is non-empty and the next color is k then one can push it almost to the center, and use the following variant of (3.32):

(3.33)

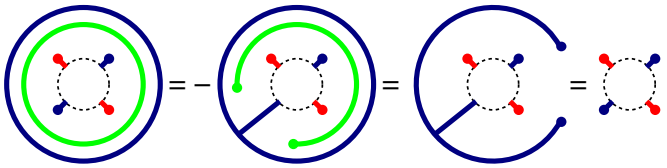

In this picture, green is $k-1$, and is the only thing in the way of the blue circle. The first equality uses (3.5), and the second equality uses (2.24), and eliminates the terms which vanish due to (3.29).

Continuing, if the decreasing sequence is empty and the next color is k then we may use (3.30) as above. Any colors which are $\geq k+1$ do not depend on the increasing sequence, and instead use the exact analogs for the increasing sequence.

Hence, in any case in which the next color appearing is not $i+1$, or $j-1$, or the beginning of a new increasing/decreasing series, we may simplify the diagram to ignore the new circle. Induction for the win. □

Therefore, the resulting diagram is equal to $z_{i,j,\underline{\boldsymbol{i}}}$, matching up either with (3.24) or (3.27).

Since every possible graph can be reduced to a form which is demonstrably in the ideal generated by $z_{i,j,\underline{\boldsymbol{i}}}$, we have proven that these elements do in fact generate the TL ideal $I_{\underline{\boldsymbol{i}}}$.

4. Some Representations

In this section, we may vary the number of strands appearing in the Temperley-Lieb algebra. When $\mathcal{TL}$ appears it designates the Temperley-Lieb algebra on $n+1$ strands, but $\mathcal{TL}_k$ designates the algebra on k strands.

4.1. **Cell Modules.** The Temperley-Lieb algebra has the structure of a cellular algebra, a concept first defined by Graham and Lehrer [8]. We will not go into detail on cellular algebras here, because for $\mathcal{TL}$ everything can be described pictorially.

One feature of cellular algebras is that they are equipped with certain modules known as *cell modules*. Cell modules provide a complete set of non-isomorphic irreducibles when the algebra is semisimple (as is the case for $\mathcal{TL}$ with generic t), and can be used to understand irreducibles even when the algebra is not semisimple. They come equipped with a basis and a bilinear form, making them obvious candidates for categorification.

Let us describe them topologically. A (n,m) *diagram* is a 1-manifold embedded on the planar strip whose boundary consists of n bottom points and m top points. This is a crossingless matching which may have additional circles. These can be partitioned by the number of *through-strands* there are in each diagram, that is, the number of strands which match a bottom endpoint to a top endpoint. Any (n,m) diagram with k through-strands can be expressed as the concatenation of a (n,k) diagram with a (k,m) diagram, and if there were no circles in the original diagram, this decomposition is unique. A (n,k) diagram with exactly k through-strands (i.e. all k of the top strands go to the bottom) and no circles is called a *cap diagram*, since it has an isotopy representative with only caps, and no cups. The vertical flip of this is called a (k,n) *cup diagram*.

The number of through strands in a diagram in $\mathcal{TL}_{n+1}$ always has the same parity as $n+1$, and we alternate between labelling diagrams by k, the number of through strands, or l, where $k = n+1-2l$. Let $l_{\max} = \lfloor \frac{n+1}{2} \rfloor$. The letters k and l always represent these labels henceforth.

Let X be the set of all $(n+1, n+1)$ crossingless matchings (i.e. no circles). Let ω be the endomorphism of X sending each diagram to its vertical flip. We will write the operation on diagrams of vertical concatenation by $\circ$: $a \circ b$ places a on top of b. Let

X_k or X^l be the set of crossingless matchings with exactly k through-strands. Let M_k or M^l be the set of all $(n+1,k)$ cap diagrams, identified with the set of all $(k,n+1)$ cup diagrams via ω.

Given a $(n+1,k)$ cap diagram a and a $(k,n+1)$ cup diagram z, there are two things we can do: take the composition $z \circ a$ to obtain an element called $c_{z,a}$ of X_k; or take the composition $a \circ z$ to get an element of $\mathcal{TL}_k$ (there may be additional circles created, and the final diagram may have fewer than k through-strands). Both compositions have the same closure on the punctured plane. Note that $\omega(c_{z,a}) = c_{\omega(a),\omega(z)}$.

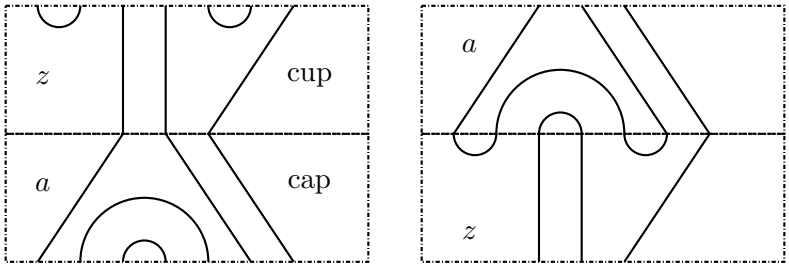

Let L_k or L^l be free $\mathbb{Z}[t,t^{-1}]$-modules spanned by M_k, the $(n+1,k)$ cap diagrams. We place a right $\mathcal{TL}$-module structure on L_k by concatenation, where circles become factors of $[2]$ as usual, and any resulting diagram with fewer than k through-strands is sent to 0. This is the *cell module* for cell k, and it is irreducible.

Example 4.1. The top cell module $L_{n+1} = L^0$ has rank 1 over $\mathbb{Z}[t,t^{-1}]$, and its generator is killed by all u_i, so that it is the quotient of $\mathcal{TL}$ by the ideal generated by all u_i.

Example 4.2. The next cell module L^1 has rank n over $\mathbb{Z}[t,t^{-1}]$, having generators v_i, $i = 1 \dots n$, such that $v_j u_i$ is equal to $[2]\, v_j$ if $i = j$, v_i if i and j are adjacent, and 0 if i and j are distant.

There is, up to rescaling, a unique pairing $(,)\colon L_k \times L_k \to \mathbb{Z}[[t,t^{-1}]]$ for which u_i is self-adjoint, that is $(au_i, b) = (a, bu_i)$. Given cap diagrams a and b in L_k, the composition $f_{a,b} = b \circ \omega(a)$ is in $\mathcal{TL}_k$. Choosing a trace ε on $\mathcal{TL}_k$ which is supported on diagrams with nesting number k (unique up to rescaling), we let $(a,b) = \varepsilon(f_{a,b})$. Alternatively, one could choose a trace on $\mathcal{TL}_{n+1}$ supported on nesting number k, and take $\varepsilon(c_{\omega(a),b})$.

4.2. **Induction from the Top Cell Module.** In order to categorify the cell modules, it will be more convenient to categorify various inductions of top cell modules.

Categorifying the top cell module L_{n+1} is simple. The module is actually a quotient of $\mathcal{TL}$ by the ideal generated by all u_i, and is one-dimensional. It is equivalent to the "sign" representation of the Hecke algebra. If we take the quotient of $\mathcal{TLC}$ by all nonempty diagrams, we get a category where the only nonzero morphism space is the one-dimensional space $\mathrm{HOM}(\emptyset,\emptyset)$. This clearly categorifies L_{n+1}, and we will say no more.

Taking the inclusion $\mathcal{TL}_J \to \mathcal{TL}$ for some sub-Dynkin diagram J, we can induce the top cell module of $\mathcal{TL}_J$ up to $\mathcal{TL}$. This is the quotient of $\mathcal{TL}$ by the right ideal generated by $u_i, i \in J$. In a future paper we will describe, for both the Hecke and Temperley-Lieb algebras, a diagrammatic way to categorify the induction of both the "sign" and "trivial" representations of sub-Dynkin diagrams, but for this paper we restrict to a specific case. If we choose the sub-Dynkin diagram J which contains every index except i, and let I_i be the corresponding ideal (generated by u_j for $j \neq i$) then we can embed L^l inside $\mathcal{TL}/I_i$ for $l = \min(i, n+1-i)$. We will categorify both $\mathcal{TL}/I_i$ and L^l accordingly.

We define a module V^i over $\mathcal{TL}$, and then prove that this module is isomorphic to $\mathcal{TL}/I_i$. This gives a way of showing that the quotient is not too small.

Let $l_i = \min(i, n+1-i)$. For $0 \leq l \leq l_i$ (and letting $k = n+1-2l$ as always), consider the following $(k, n+1)$ cup diagram a_k^i, where the innermost cup is always in position i:

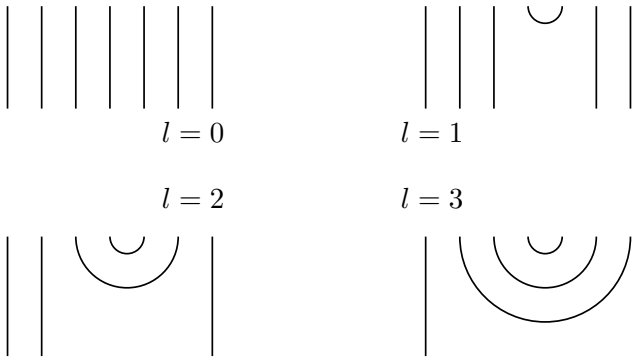

Let $X_k^i \subset X_k$ consist of all matchings of the form $c_{a_k^i, b}$ for $b \in M_k$. Let X^i be the disjoint union of all X_k^i for $0 \leq l \leq l_i$, and let V^i be the free $\mathbb{Z}[t, t^{-1}]$-module with basis X^i. There is a distinguished element $\mathbb{1}$ of this basis, the unique member of X_{n+1}^i. If one viewed elements of X^i as though they were in $\mathcal{TL}$, it is not hard to check that they correspond exactly to those words $u_{\underline{i}}$ where *every* presentation of the word begins with u_i. This motivates the definition.

Let $\mathcal{TL}$ act on V^i on the right by viewing elements of V^i as though they were in $\mathcal{TL}$, using the standard multiplication rules, and then ignoring any terms whose diagrams are not in X^i. While something does need to be checked to ensure that this defines a module action, it is entirely straightforward. In the Temperley-Lieb algebra, things are generally easy to prove because products of monomials always reduce to another monomial (with a scalar), not a linear combination of multiple monomials. Therefore, checking the associativity condition for being a module, say, involves showing that both sides of an equation are the same diagram in X^i, or that both sides are 0. This module is cyclic, generated by $\mathbb{1}$, and I_i is clearly in the annihilator of $\mathbb{1}$, so that $\mathcal{TL}/I_i$ surjects onto V^i. By counting dimensions it is clear that $\mathcal{TL}/I_i$ is no bigger than V^i, so they must be isomorphic.

There is a cellular filtration on V^i, given by the span of diagrams with $\leq k$ through-strands (call it V^i_k). Clearly, each subquotient in this filtration is generated by the elements $c_{a^i_k,b}$ for $b \in M_k$, and it is an easy exercise that this subquotient is isomorphic to the cell module L_k. There is one subquotient for each $0 \leq l \leq l_i$, and when l_i, we see that $L^{l_i} \cong V^i_{n+1-2l}$ is a submodule of V^i.

Since i may be any number from 1 to n, every possible nonzero value of l_i is obtained up to $l_{\max}$, and every cell module except the trivial cell module $L_{n+1} = L^0$ is obtained as a submodule of some V^i.

Claim 4.3. *Consider the $\mathbb{Z}[[t,t^{-1}]]$-module of semi-linear pairings on V^i where $(xu_j, y) = (x, yu_j)$ for all j. Consider the $l_i + 1$ functionals on this space, which send a pairing to $(\mathbb{1}, c_{a^i_k,\omega(a^i_k)})$. Then these linear functionals are independent and yield an isomorphism between the space of pairings and a free module of rank $l_i + 1$.*

Note that, using adjointness, one can check that $[2]^l(\mathbb{1}, c_{a^i_k,\omega(a^i_k)}) = (c_{a^i_k,\omega(a^i_k)}, c_{a^i_k,\omega(a^i_k)})$.

Proof. Given diagrams $x, y \in X^i$, the adjointness of u_i implies that the value of (x, y) is an invariant of the diagram $y \circ \omega(x)$. In particular, $(x, y) = (\mathbb{1}, y\omega(x)) = (x\omega(y), \mathbb{1})$, where $y\omega(x)$ refers to the image of this diagram in the quotient $\mathcal{TL}/I_i$. Therefore, if either $y\omega(x)$ or $x\omega(y)$ is not in X^i then the value of (x, y) is zero. However, $X^i \cap \omega(X^i) = \{c_{a^i_k,\omega(a^i_k)}\}$ where this set runs over all k with $0 \leq l \leq l_i$. Thus the value of the pairing on all elements is clearly determined by the values of $(\mathbb{1}, c_{a^i_k,\omega(a^i_k)})$ for all such k.

To show independence, we need only construct $l_i + 1$ independent pairings on V^i which distinguish these values. This amounts to showing that the following is actually a well-defined pairing: fix k, and for basis elements x, y send (x, y) to $r \in \mathbb{Z}[t,t^{-1}]$ if $y\omega(x) = rc_{a^i_k,\omega(a^i_k)} \in \mathcal{TL}$, and send (x, y) to zero otherwise. Clearly this is a well-defined $\mathbb{Z}[t,t^{-1}]$-module map and u_j is self-adjoint. This suffices. □

Remark 4.4. Once again, all pairings are defined topologically. The element $c_{a^i_k,\omega(a^i_k)}$ has nesting number exactly k, which distinguishes the traces.

4.3. **Categorifying Cell Modules.** Consider the quotient of the category $\mathcal{TLC}$ by all diagrams where any color not equal to i appears on the left. Call this quotient $\mathcal{V}^i$. We claim that $\mathcal{V}^i$ categorifies V^i. Not only this, but the action of $\mathcal{TLC}$ on $\mathcal{V}^i$ by placing diagrams on the right will categorify the action of $\mathcal{TL}$ on V^i.

Clearly, any monomial $u_{\underline{\boldsymbol{i}}}$ which goes to zero in V^i will correspond to an object $U_{\underline{\boldsymbol{i}}}$ whose identity morphism is sent to zero in $\mathcal{V}^i$, since it is isomorphic to an object $U_{\underline{\boldsymbol{j}}}$ where some color not equal to i occurs on the far left in $\underline{\boldsymbol{j}}$. It is essentially obvious that there is a *surjective* map from V^i to the Grothendieck group of $\mathcal{V}^i$, and that the action of $\mathcal{TLC}$, descended to the Grothendieck group, will commute with the action of $\mathcal{TL}$ on V^i under this surjective map.

Therefore, HOM spaces in $\mathcal{V}^i$ will induce a semi-linear pairing on V^i, which satisfies the property $(au_j, b) = (a, bu_j)$ because U_j is self-adjoint. As before, once we determine which pairing this is, our proof will be almost complete.

Lemma 4.5. *The pairing induced by $\mathcal{V}^i$ will satisfy $(\mathbb{1}, c_{a_k^i,\omega(a_k^i)}) = \frac{t^l}{1-t^2}$ where $k = n+1-2l$.*

Remark 4.6. Taking a $(n+1, n+1)$ diagram and closing it off on the punctured plane, if m is the number of circles and k is the nesting number, then the pairing comes from the trace on $\mathcal{TL}$ which sends this configuration to $[2]^{l+m-(n+1)} \frac{t^l}{1-t^2}$.

For a closure of an arbitrary diagram, $l + m < n + 1$ is possible. However, for any diagram in $X^i \cap \omega(X^i)$ (with extra circles thrown in) we have $l + m \geq n + 1$, since removing the circles yields precisely $c_{a_k^i,\omega(a_k^i)}$ for some k. This guarantees that evaluating the formula on an element of V^i yields a power series with *non-negative* coefficients.

Theorem 4. *$\mathcal{V}^i$ is idempotent closed and has Krull-Schmidt. Its Grothendieck group is isomorphic to V^i.*

Proof. It is enough to check that for any $u_{\underline{\boldsymbol{i}}} \neq u_{\underline{\boldsymbol{j}}}$ corresponding to matchings in X^i, that $\mathrm{HOM}(U_{\underline{\boldsymbol{i}}}, U_{\underline{\boldsymbol{i}}})$ is concentrated in non-negative degrees with a 1-dimensional degree 0 part, and that $\mathrm{HOM}(U_{\underline{\boldsymbol{i}}}, U_{\underline{\boldsymbol{j}}})$ is concentrated in strictly positive degrees. This is a calculation using the semi-linear pairing. We assume the lemma.

Letting m be the number of circles in a configuration on the punctured disk, and $k = n + 1 - 2l$ the nesting number, then the evaluation will be in strictly positive degrees if $m < n+1$, and will be in non-negative degrees with a 1-dimensional degree 0 part if $m = n+1$ exactly. But this was precisely the calculation in the proof of Lemma 3.3: for arbitrary crossingless matchings $u_{\underline{\boldsymbol{i}}}$ and $u_{\underline{\boldsymbol{j}}}$, the closure of $u_{\underline{\boldsymbol{i}}}\omega(u_{\underline{\boldsymbol{j}}})$ has fewer than $n + 1$ circles if $u_{\underline{\boldsymbol{i}}} \neq u_{\underline{\boldsymbol{j}}}$, and exactly $n + 1$ if they're equal. □

Corollary 4.7. *Let $\mathcal{L}^{l_i}$ be the full subcategory of $\mathcal{V}^i$ with objects consisting of $U_{\underline{\boldsymbol{i}}}$ such that $u_{\underline{\boldsymbol{i}}}$ is an element of $V^i_{n+1-2l_i}$. This has an action of $\mathcal{TLC}$ on the right. On the Grothendieck group, this setup categorifies the cell module $L^{l_i} = V^i_{n+1-2l_i}$.*

Proof. That this subcategory is closed under the action of $\mathcal{TLC}$ is obvious, as is the existence of a surjective map from L^{l_i} to the Grothendieck group. We already know the induced pairing, because the subcategory is full. Therefore the same arguments imply that the Grothendieck group behaves as planned. □

Proof of Lemma 4.5. To calculate the pairing, we may calculate $(u_{\underline{\boldsymbol{i}}}, u_{\underline{\boldsymbol{i}}}) = \mathrm{gdimEND}(U_{\underline{\boldsymbol{i}}})$ for the following choices of $\underline{\boldsymbol{i}}$: $\emptyset$, i, $i(i+1)(i-1)$, $i(i+1)(i-1)(i+2)i(i-2)$, $i(i+1)(i-1)(i+2)i(i-2)(i+3)(i+1)(i-1)(i-3)$, etc. These are pictured below.

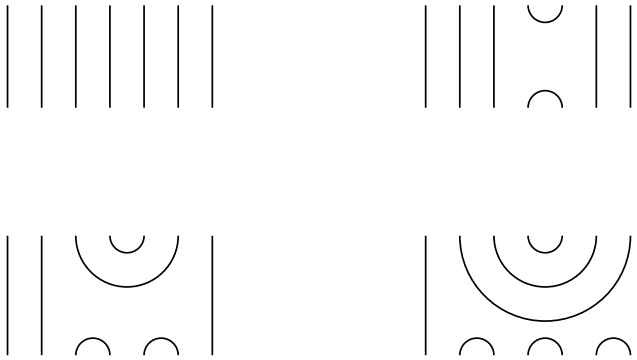

These sequences are split into subsequences we call "tiers", where the mth sequence adds the mth tier. The following property of these sequences is easily verified: each sequence $\underline{\boldsymbol{i}}$ is in X^i, and remains in X^i if one removes any subset of the final tier, but ceases to be in X^i if one removes a single element from any other tier instead. Fixing $\underline{\boldsymbol{i}}$ nonempty in this sequence, let $\underline{\boldsymbol{j}}$ be the subsequence with the final tier removed.

We wish to show that $\mathrm{gdimEND}(U_{\underline{\boldsymbol{i}}}) = \frac{(1+t^2)^l}{1-t^2}$. Note that l is exactly the number of elements in the final tier. We let blue represent the color i.

Now consider an element of the endomorphism ring. Using previous results, we may assume it is a simple forest, with all double dots on the far left. Any double dot colored $j \neq i$ will be sent to zero, so we have only an action of the ring $\Bbbk[f_i]$ on the left. This accounts for the $\frac{1}{1-t^2}$ appearing in all the formulae.

Suppose there is a boundary dot in the morphism on any line not in the final tier. Then the morphism factors through the sequence $U_{\underline{\boldsymbol{k}}}$ where $\underline{\boldsymbol{k}}$ is $\underline{\boldsymbol{i}}$ with that index removed. As discussed above, $u_{\underline{\boldsymbol{k}}}$ is not in X^i and therefore $U_{\underline{\boldsymbol{k}}}$ is isomorphic to the zero object. See the first picture below for an intuitive reason why such a morphism vanishes. Hence the only boundary dots which can appear occur on the final tier. It is easy to check that the existence of a trivalent vertex joining three boundary lines will force the existence of a dot not on the final tier. See the second picture below. Both pictures are for the sequence $i(i+1)(i-1)(i+2)i(i-2)$.

Therefore, we must have $\mathbb{1}_{U_{\underline{\boldsymbol{j}}}}$, accompanied on the right by either identity maps or broken lines (pairs of boundary dots), because all other simple forests yield a zero map. Identity maps have degree zero, while broken lines have degree 2. If these pictures form a basis (along with the action of blue double dots on the left), then the graded dimension will be exactly as desired. An example with $l = 3$, two broken lines, and one unbroken line is shown below.

This spanning set is linearly independent in $\mathcal{TLC}$ over $\Bbbk$, so any further dependencies must come from having a non-blue color on the left. Consider an arbitrary endomorphism, and reduce it using the $\mathcal{TLC}$ relations to a simple forest with all double dots on the left. The actual double dots appearing are ambiguous, since there are polynomial relations in $\mathcal{TLC}$, but it is easy (knowing the generators of the TL ideal) to note that these relations are trivial modulo non-blue colors. Hence the spanning set will be linearly independent if any diagram in $\mathcal{TLC}$ which started with a non-blue color on the left will still have a non-blue color (perhaps in a double-dot) on the left after reducing to a simple forest. This will be the case for any diagram with a boundary dot on $\underline{\boldsymbol{j}}$.

Let red indicate any other index, and suppose that red appears on the far left. Regardless of what index red is, unless there is a dot on $\underline{\boldsymbol{j}}$, the identity lines of $\underline{\boldsymbol{j}}$ block this leftmost red component from reaching any red on the boundary of the graph. Take a neighborhood of a red line segment which includes no other colors and goes to $-\infty$. Excising this neighborhood, we get a simply-connected region where the only relevant red boundary lines are the two which connect to the ends of the segment. Red then will reduce to a simple forest with double dots on the left, which in this case yields either a red double dot or a red circle (potentially with more double dots).

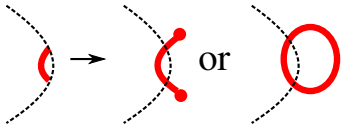

However, no colors adjacent to red can interfere on the interior of a red circle, so the circle evaluates to zero. Therefore, the diagram evaluates to zero or has at least one red double dot on the left. We may ignore the red double dot and reduce the remainder of the diagram, and so regardless of what else is done, the final result will have a red double dot on the left. □

References

[1] G. Bergman, The diamond lemma for ring theory, *Advances in Math.* **29** (1978), 178-218.

[2] J. Bernstein, I. B. Frenkel, and M. Khovanov, A categorification of the Temperley-Lieb algebra and Schur quotients of $U(\mathfrak{sl}_2)$ via projective and Zuckerman functors, *Selecta Math. (N.S.)* **5**, no.2 (1999), 199-241.

[3] D. Bar-Natan, Khovanov's homology for tangles and cobordisms, *Geom. Topol.* **9** (2005), 1443–1499

[4] J. Chuang and R. Rouquier, Derived equivalences for symmetric groups and sl_2-categorification, 2004, math.RT/0407205v2.

[5] B. Elias, Lecture notes on traces on the Hecke and Temperley-Lieb algebras, http://www.math.columbia.edu/∼belias/papers/Traces.pdf.

[6] B. Elias and M. Khovanov, Diagrammatics for Soergel categories, 2009, math.QA/0902.4700.

[7] B. Elias and D. Krasner, Rouquier complexes are functorial over braid cobordisms, 2009, math.RT/0906.4761.

[8] J. J. Graham and G. I. Lehrer, Cellular algebras, *Invent. Math.* **123**, (1996) 1–34.

[9] L. Kauffman, State models and the Jones polynomial, *Topology* **26** (1987), no. 3, 395–407

[10] M. Khovanov, A functor-valued invariant of tangles, *Algebr. Geom. Topol.* **2** (2002), 665–741

[11] M. Khovanov and A. Lauda, A diagrammatic approach to categorification of quantum groups I, *Represent. Theory* **13** (2009), 309–347, also arXiv:0803.4121.
[12] M. Khovanov and A. Lauda, A diagrammatic approach to categorification of quantum groups III, arXiv:0807.3250.
[13] A. Lauda, Categorified quantum sl(2) and equivariant cohomology of iterated flag varieties, 2008, arXiv:0803.3848.
[14] A. Lauda and M. Vazirani, Crystals from categorified quantum groups, 2009, math.RT/0909.1810.
[15] R. Rouquier, Categorification of the braid groups, math.RT/0409593.
[16] R. Rouquier, Categorification of sl_2 and braid groups, in *Trends in Representation Theory of Algebras and Related Topics (Querétaro, Mexico, 2004), Contemp. Math.* **406**, AMS, Providence, 2006, 137–167.
[17] R. Rouquier, 2-Kac Moody algebras, math.RT/0812.5023.
[18] W. Soergel, The combinatorics of Harish-Chandra bimodules, *Journal Reine Angew. Math.* **429**, (1992) 49–74.
[19] W. Soergel, Gradings on representation categories, *Proceedings of the ICM 1994 in Zürich*, 800–806, Birkhäuser, Boston.
[20] W. Soergel, Combinatorics of Harish-Chandra modules, *Proceedings of the NATO ASI 1997, Montreal, on Representation theories and Algebraic geometry*, edited by A. Broer, Kluwer (1998).
[21] W. Soergel, Kazhdan-Lusztig-Polynome und unzerlegbare Bimoduln über Polynomringen, math.RT/0403496v2, english translation available on the author's webpage.
[22] W. Soergel, On the relation between intersection cohomology and representation theory in positive characteristic, *Journal of Pure and Applied Algebra* **152** (2000), 311–335.
[23] C. Stroppel, Categorification of the Temperley-Lieb category, tangles, and cobordisms via projective functors, *Duke Math. Journal* **126** (3), (2005) 547–596.
[24] M. Varagnolo and E. Vasserot, Canonical bases and Khovanov-Lauda algebras, 2009, math.RT/0901.3992
[25] P. Vaz. The diagrammatic Soergel category and sl(2) and sl(3) foams, 2009, math.QA/0909.3495.
[26] B. Webster, Knot invariants and higher representation theory, 2010, math.GT/1001.2020
[27] B. W. Westbury, The representation theory of the Temperley-Lieb algebras, *Mathematische Zeitschrift* **219**, (1995) 539–566.

Ben Elias, Department of Mathematics, Columbia University, New York, NY 10027
email: belias@math.columbia.edu